Arteriosclerosis, Thrombosis, and Vascular Biology

BASIC SCIENCES

Meta-Analysis of Single-Cell RNA-Seq Data Reveals the Mechanism of Formation and Heterogeneity of Tertiary Lymphoid Organ in Vascular Disease

Xuejing Sun,* Yao Lu,* Junru Wu,* Qing Wen, Zhengxin Li, Yan Tang, Yunmin Shi, Tian He, Lun Liu, Wei Huang, Chunyan Weng, Qing Wu, Qingzhong Xiao, Hong Yuan, Qingbo Xu, Jingjing Cai

BACKGROUND: Tertiary lymphoid organs (TLOs) are ectopic lymphoid organs developed in nonlymphoid tissues with chronic inflammation, but little is known about their existence in different types of vascular diseases and the mechanism that mediated their development.

METHODS: To take advantage of single-cell RNA sequencing techniques, we integrated 28 single-cell RNA sequencing data sets containing 5 vascular disease models (atherosclerosis, abdominal aortic aneurysm, intimal hyperplasia, isograft, and allograft) to explore TLOs existence and environment supporting its growth systematically. We also searched Medline, Embase, PubMed, and Web of Science from inception to January 2022 for published histological images of vascular remodeling for histological evidence to support TLO genesis.

RESULTS: Accumulation and infiltration of innate and adaptive immune cells have been observed in various remodeling vessels. Interestingly, the proportion of such immune cells incrementally increases from atherosclerosis to intimal hyperplasia, abdominal aortic aneurysm, isograft, and allograft. Importantly, we uncovered that TLO structure cells, such as follicular helper T cells and germinal center B cells, present in all remodeled vessels. Among myeloid cells and lymphocytes, inflammatory macrophages, and T helper 17 cells are the major lymphoid tissue inducer cells which were found to be positively associated with the numbers of TLO structural cells in remodeled vessels. Vascular stromal cells also actively participate in vascular TLO genesis by communicating with myeloid cells and lymphocytes via CCLs (C-C motif chemokine ligands), CXCL (C-X-C motif ligand), lymphotoxin, BMP (bone morphogenetic protein) chemotactic, FGF-2 (fibroblast growth factor-2), and IGF (insulin growth factor) proliferation mechanisms, particularly for lymphoid tissue inducer cell aggregation. Additionally, the interaction between stromal cells and immune cells modulates extracellular matrix remodeling. Among TLO structure cells, follicular helper T, and germinal center B cells have strong interactions via TCR (T-cell receptor), CD40 (cluster of differentiation 40), and CXCL signaling, to promote the development and maturation of the germinal center in TLO. Consistently, by reviewing the histological images from the literature, TLO genesis was found in those vascular remodeling models.

CONCLUSIONS: Our analysis showed the existence of TLOs across 5 models of vascular diseases. The mechanisms that support TLOs formation in different models are heterogeneous. This study could be a valuable resource for understanding and discovering new therapeutic targets for various forms of vascular disease.

GRAPHIC ABSTRACT: A graphic abstract is available for this article.

Key Words: allografts ■ endothelial cells ■ isografts ■ meta-analysis ■ vascular remodeling

Correspondence to: Qingbo Xu, MD, Department of Cardiology, The First Affiliated Hospital, Zhejiang University, 79 Qingchun Rd, Hangzhou 310003, Zhejiang, China, Email qingbo_xu@zju.edu.cn; or Jingjing Cai, MD, Department of Cardiology, The Third Xiangya Hospital of Central South University, 138 Tong-Zi-Po Rd, Changsha, Hunan, 410013, China, Email caijingjing83@hotmail.com, caijingjing@csu.edu.cn
*X. Sun, Y. Lu, and J. Wu contributed equally and shared first authorship.
Supplemental Material is available at https://www.ahajournals.org/doi/suppl/10.1161/ATVBAHA.123.318762.
For Sources of Funding and Disclosures, see page 1884.

Arterioscler Thromb Vasc Biol is available at www.ahajournals.org/journal/atvb

Nonstandard Abbreviations and Acronyms

AAA	abdominal aortic aneurysm
ApoE$^{-/-}$	apoE knockout
BCR	B-cell receptor
BMP	bone morphogenetic protein
CCL2	C-C motif chemokine ligand 2
CD40	cluster of differentiation 40
CXCL	C-X-C motif ligand
DC	dendritic cell
DZ	dark zone
EC	endothelial cell
FGF	fibroblast growth factor
FITC	fluorescein isothiocyanate
FoxO1	forkhead box O1
GC	germinal center
IH	intimal hyperplasia
IL	interleukin
LDL$^{-/-}$	low-density lipoprotein knockout
LTβR	LTβ receptor
LT	lymphotoxin
LTi	lymphoid tissue inducer
LZ	light zone
MK	mitogen-activated protein kinases
PSAP	prostatic serum acid phosphatase
PTN	pleiotrophin
scRNA-seq	single-cell RNA sequencing
SMC	smooth muscle cell
TCR	T-cell receptor
Tfh	follicular helper T cells
TGF	transforming growth factor
Th	T helper cells
TLO	tertiary lymphoid organ
TNF	tumor necrosis factor

Highlights

- Vascular remodeling involves inflammatory response and complex cellular networks that change the geometry of the blood vessel.
- Both innate and adaptive immune responses are involved in various vascular diseases.
- Tertiary lymphoid organs (TLOs) are ectopic lymphoid organs that develop in nonlymphoid tissues at sites of chronic inflammation.
- TLOs are present in remodeled vessels and the mechanisms mediating TLO formation vary by vascular pathologies.
- Inflammatory macrophages and T helper 17 cells are the major lymphoid tissue inducer cells in remodeled vessels. The lymphoid tissue inducer cells are attracted by stromal cells to the site of inflammation via a chemotactic mechanism.
- The levels of inflammatory responses in lymphoid tissue inducer cells are tightly associated with the numbers of TLO structural cells (ie, follicular helper T cells and germinal center B cells) at the late stage of vascular remodeling.
- Vascular stromal cells, including endothelial cells, smooth muscle cells, fibroblast, and mesenchymal stem cells, also actively participate in vascular TLO genesis by communicating with myeloid cells and lymphocytes. In addition to strong chemotactic effects, vascular tissues are shaped by such communication through extracellular matrix remodeling.
- TLO structure cells, including the follicular helper T cells and germinal center B cells, interact tightly via TCR (T-cell receptor), CD40 (cluster of differentiation 40), and CXCL (C-X-C motif ligand) signaling, to promote the development and maturation in the germinal center.
- Our results can serve as a resource for a deeper understanding of vascular TLO formation and may provide valuable insights for new therapeutic strategies targeting various forms of vascular injury.

Vascular remodeling is a broad term that includes cardiovascular diseases like atherosclerosis, arterial aneurysm, and intimal hyperplasia (IH) after vascular intervention and bypass surgery.[1] Such active processes involve a complex cellular network that changes the geometry of the blood vessel.[2] Accumulating evidence has shown that both innate and adaptive immune cells infiltrate into vascular and perivascular tissue to play important roles in modulating local inflammation and vascular remodeling.[3–10] In addition to diffuse perivascular infiltrates, recent discoveries have shown that heterogeneous immune cells form organized local tertiary lymphoid organs (TLOs) in response to various inflammatory signals from the vascular microenvironment.[11] However, the precise mechanism and function of TLO in vascular remodeling have not been fully established.

TLOs are ectopic lymphoid organs that develop in nonlymphoid tissues at sites of chronic inflammation, including tumors, autoimmune diseases, and transplanted organs.[12] Typical TLOs are composed of a T-cell–rich zone with mature dendritic cells (DCs) juxtaposing a B-cell follicle with germinal center (GC) characteristics and are surrounded by plasma cells.[13] Specialized vessels in this structure termed high endothelial venules allow entry of lymphocytes into TLOs. TLO is a highly active site for recruited naive T-cell and B-cell differentiation and activation into effector T cells and B cells under the exposure of neighboring antigens and cofactors, including cytokine and chemokine.[14] In different diseases, their presences are associated with different outcomes and prognoses. For example, in tumors, TLO

 Arterioscler Thromb Vasc Biol. 2023;43:1867–1886. DOI: 10.1161/ATVBAHA.123.318762

can induce a long-lasting antitumor response and is associated with a favorable prognosis in solid tumors.[15] In patients with lupus nephritis, the presence of TLO has been increasingly recognized to be associated with poorer renal outcomes.[16] Importantly, emerging evidence shows the existence of TLOs surrounding atherosclerotic lesions, which are tightly associated with the progression of lesions.[17–20] Recently, our group also found the local formation of TLOs in transplant arteriosclerosis, and their presence is detrimental to the long-term survival of solid organs.[21] Thus, understanding the pathological mechanisms of TLOs may yield novel therapeutic targets for controlling vascular remodeling.

In this study, integrated published and newly generated single-cell RNA sequencing (scRNA-seq) data, we mapped the structure cells of TLOs across 5 vascular remodeling models, including atherosclerosis, abdominal aortic aneurysm (AAA), wire injury–induced IH, isograft, and allograft artery remodeling. The mechanisms that support TLO formation and their heterogeneities in different models were also characterized. We also systemically reviewed vascular remodeling studies and obtained direct evidence of histological images that supports TLO genesis. This study could be valuable resource for understanding and discovering new therapeutic targets of various forms of vascular disease.

METHODS

Data Availability

The data that support the findings of this study are available from the corresponding author on reasonable request. scRNA-seq data of our study are available in Gene Expression Omnibus (GSE234651 for scRNA-seq of carotid artery wire injury IH model). Publicly available data obtained from mouse and human subjects were analyzed, and the data sets involved in this study and details of the scRNA-seq data are available in the public domain as outlined in Table S10.

Meta-Analysis and Data Acquisition

A comprehensive meta-analysis of the atlas for scRNA sequencing studies involving 5 data sets of healthy mouse vessels and 28 data sets of remodeling vessels was performed. Each raw data set was derived from the Gene Expression Omnibus (Figure 1A). The workflow for the collection of data sets of interest is summarized in Figure 1A and 1B. Briefly, the data sets of remodeling vessels included (1) 14 atherosclerotic arterial data sets containing gene-induced (eg, apoE knockout [*ApoE*$^{-/-}$] and *Ldlr*$^{-/-}$ mice) and high-fat diet–induced mouse atherosclerosis; (2) 2 data sets of elastase-induced aneurysm remodeling vessels; (3) 2 data sets of surgical model–induced vascular remodeling after mechanical injury; and (4) 5 data sets of surgical model–induced isograft and allograft remodeling vessels. Details of these data sets and cells harvested for single-cell sequencing are presented in Table S10.

Inclusion and Exclusion for Mice Data Sets

We conducted a systematic search of the uploaded data sets in the Gene Expression Omnibus database in January 2022.

Inclusion Criteria

Database: Gene Expression Omnibus database.
MeSH terms: atherosclerosis, aneurysm, hyperplasia, isograft, and allograft.
Species: *Mus musculus*.
Dates: from inception to January 2022.

The search terms included the following: atherosclerosis, aneurysm, hyperplasia, isograft, and allograft. Atherosclerotic models contained arteries of ApoE$^{-/-}$ or low-density lipoprotein knockout (LDL$^{-/-}$) mice fed a high-fat diet. The grafting arteries were isolated from Balb/c mice in allograft models. The healthy arteries, aneurysm, wire injury–induced hyperplasia, and isograft vasculopathies models were established on mice with C57BL6J background. Anatomic location of vessels in each disease model and cell sorting strategies are listed in Table S10.

Excluded Studies That Met the Following Criteria

Vascular data other than the abovementioned models (atherosclerosis, aneurysm, hyperplasia, isograft, and allograft) were not included. We only collected scRNA sequencing data, and the bulk RNA sequencing and sn-RNA sequencing data were excluded. Among them, the scRNA sequencing data are the data sets obtained by digesting the healthy or remodeling vessel (Figure 1B).

For the data sets in which cells were sorted (eg, sorted CD45^{+} cells), none of them were included in the analysis when calculating the proportion. However, those sorted data sets integrated with unsorted data sets when performing functional analysis or cell-cell interaction analysis for certain types of cells. No language restrictions were applied. The included data sets and studies are listed in Table S10.

Meta-Analysis Strategy

After collecting data sets that met the inclusion criteria, we first used Harmony R package to integrate multiple data sets and mitigate batch effects, as it has been proven effective in achieving harmonized data integration and reducing unwanted variation caused by batch effects.[22] Then the cell annotation was performed after data quality control by R package Seurat (version 4.3.0). Briefly, gene features expressed in at least 5 cells, and cells with at least 500 detected genes, <10% mitochondrial counts were kept. Red blood cells (expressing Alas2) were also filtered and removed. The data sets of the sorted vessel cells were not included in the analysis when calculating and comparing cell type ratios. However, those sorted data sets were included when performing other analyses. We compared the expression levels of different vital functional gene sets for TLO formation in stromal cells and immune cells in remodeling vessels with those in healthy aortas. For different cell types, more detailed analysis (such as the expression of characteristic functional gene sets, cell-cell communication analysis, etc) was further performed.

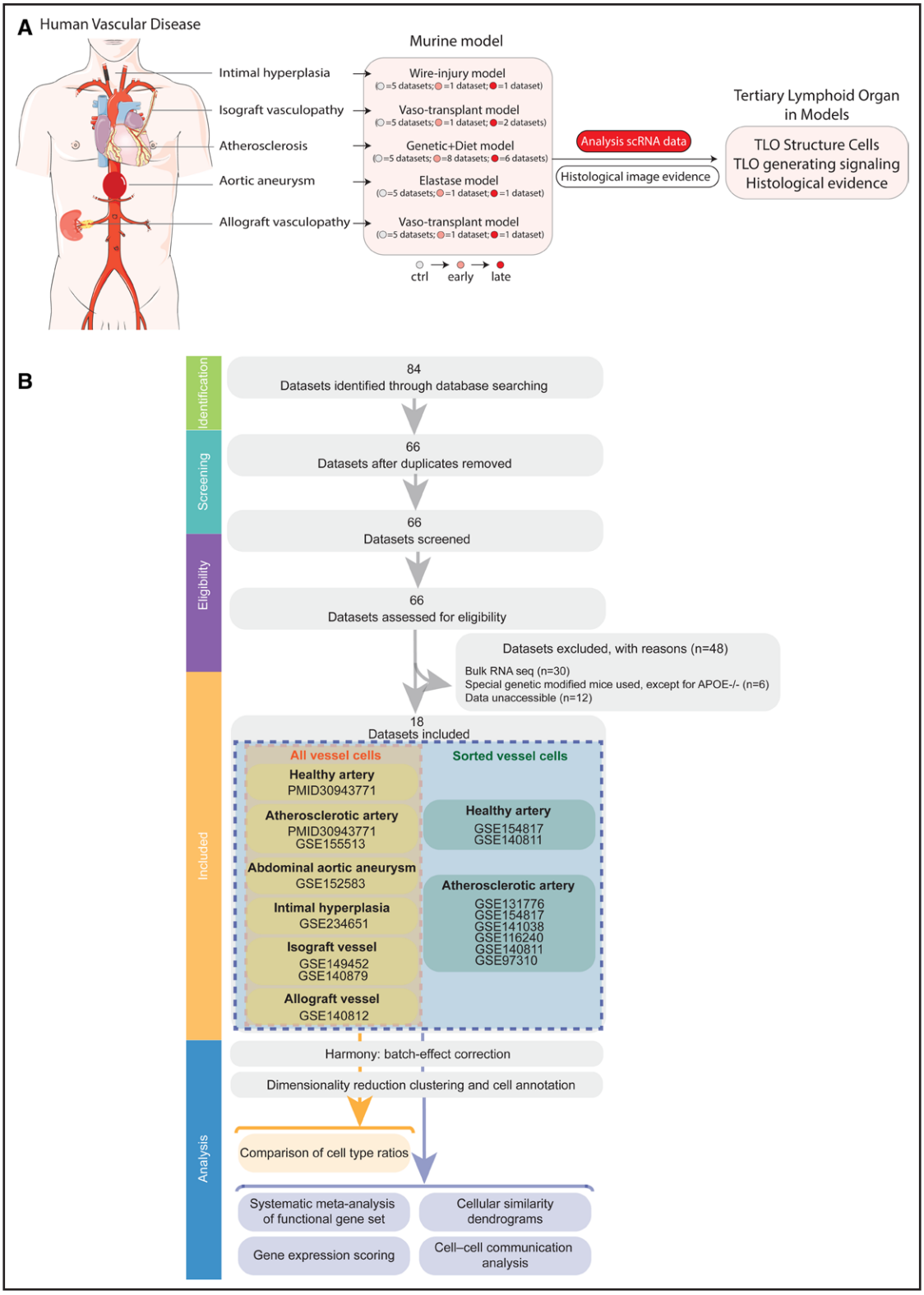

Figure 1. Design of the meta-analysis study.

A, Overview of the study. This analysis is based on 28 data sets (5 healthy artery and 23 remodeled vessel data sets, including atherosclerosis, arterial aneurysm, intimal hyperplasia after vascular intervention, and bypass surgery [including isograft and allograft data sets] from published studies in mice). Atherosclerosis was induced in mouse models using genetic knockout (low-density lipoprotein receptor knockout [$Ldlr^{-/-}$] and apoE knockout [$ApoE^{-/-}$]) and a high-fat diet model. The arterial aneurysm model was built by applying elastase to aorta in C57BL6J mice. The intimal hyperplasia model was established by introducing a flexible wire into carotid arteries and achieving an effect in endothelial denudation in C57BL6J mice. In the isograft model, C57BL6J mice received vessels from mice with same gene background. In the allograft model, C57BL6J mice received vessels from Balb/c strain. Single cells were phenotyped by RNA sequencing (RNA-seq). Dimensionality reduction (*Continued*)

 Arterioscler Thromb Vasc Biol. 2023;43:1867–1886. DOI: 10.1161/ATVBAHA.123.318762

Data Analysis and Visualization

Single-cell expression count matrix barcodes and gene IDs from each study were downloaded from the Gene Expression Omnibus. Doublet detection for those scRNA-seq data using artificial nearest neighbors was conducted via R package DoubletFinder (version 2.0.3).[23] To normalize the data, Unique Molecular Identifiers, the unique tags attached to each molecule, were used to facilitate the identification and removal of polymerase chain reaction duplicates.[21,23] Unique molecular identifier counts were scaled by library size and natural log transformation; gene counts for each cell were divided by the total unique molecular identifier count of that cell, scaled by a factor of 10 000, and then transformed via a natural log plus 1 function (NormalizeData). For downstream analysis, normalized data were additionally scaled so that the mean expression across cells was 0 and the variance was 1 (function ScaleData). To reduce the dimensionality of the data for clustering functions, principal component analysis was utilized, and we identified the first 30 principal components that explained sufficient observed variance (function RunPCA). The determination of sufficiency is based on the examination of the elbow plot (function ElbowPlot), which displays the eigenvalues of the principal components in descending order and the eigenvalues began to level off after the first 30 PCs in elbow plot. Next, to identify clusters within the reduced dimensional space, cells were embedded in a k-nearest neighborhood-based graph structure (function FindNeighbors) and were then partitioned into clusters (function FindClusters). Finally, for visualization, Uniform Manifold Approximation and Projection was run over the reduced dimensional space (function RunUMAP), and identified clusters were projected onto the Uniform Manifold Approximation and Projection plot. To address noise and batch differences between the studies, a strategy involving the use of reference cells from each data set was used. To facilitate integration, pairs of reference cells, known as anchors, were identified and scored based on their proximity using a k-nearest neighbor approach (function FindIntegrationAnchors). These anchors were then used to measure the expression difference between studies (function IntegrateData), which was then removed from the corresponding normalized data. Integration was run between the normalization and scaling steps.[24] All the functions used are based on Seurat.

Clustering was performed in Seurat. To establish the reliability of this method, the clustering algorithm was compared between Seurat and an alternative approach using the Harmony R package (https://github.com/immunogenomics/harmony)[22] This package scales the data to make nearby cells more similar when clustering is performed. Harmony is also easily incorporated into the Seurat pipeline. The results using Harmony-based clustering were essentially identical to those from the Seurat clustering. In this meta-analysis, batch effect was only corrected once in the initial data integration, and removal for batch effects was not repeatedly performed in downstream analysis.[22,25]

Cellular Similarity Dendrograms

For an unsupervised comparison of the cellular subpopulations identified from multiple vascular remodeling types, the following steps were performed.

Here, we used the batch-corrected expression value via a method named Scanorama.[26]

1. Identify a set of highly variable genes across different cellular subpopulations.
2. Calculate the mean expression of genes in each cluster.
3. For hierarchical clustering, the distance defined as (1-Pearson correlation coefficient)/2 was used.

For major myeloid lineages comparison across multiple vascular remodeling types, we used the top 1000 highly variable genes. For other subpopulations, comparison, the top 800 highly variable genes were used.

Correlation Analysis

Expression levels were averaged over cells and plotted among cell types in Figures 2H, 3G, 4H, and 5E. Scatter plots were fit with linear and quadratic regression models to show potential relationships. The correlation was assessed via scatter plots and Spearman correlation coefficient.[26]

Differentially Expressed Genes

The features of differentially expressed genes in the cell clusters (or subclusters) in all scRNA-seq analyses were identified with the Seurat function FindAllMarkers, with a minimum log2 (fold change) threshold of 0.25, a minimum of 0.25 fractions in cells, and an adjusted P value of <0.05. P values were calculated based on a Wilcoxon rank-sum test and adjusted with the Benjamini-Hochberg procedure.

Gene Sets

The Seurat function AddModuleScore includes genes related to proinflammatory signaling, antigen presentation, lymphatics, chemokines, cytokines, MHCI, MHCII, follicular helper T-cell (Tfh)–like cells, and Tfh cell differentiation.[4] Each cell was scored based on its expression of the genes within the gene sets. The gene sets are shown in Table S2.

Pathway Enrichment Analysis

Differentially expressed gene data sets were loaded into R for Gene Ontology term enrichment analysis. For the pathway enrichment analyses, R package gProfileR2 (version 0.2.1)

Figure 1 Continued. and clustering were used to identify cell types and gene signatures. Based on the gene signatures, genetic labeling was used to visualize and sort cell types to gain functional insights and in-depth transcriptome information. Pathological analysis of the histological images collected from published articles was performed and vascular–tertiary lymphoid organ (TLO) immunofluorescent staining for each model was provided. The study focused on cellular diversity and TLO formation in vascular remodeling. **B**, Flowchart showing the procedure for the meta-analysis study. Only single-cell RNA sequencing (scRNA-seq) data were collected, and the bulk RNA sequencing and sn-RNA sequencing data were excluded. The included studies were limited by mice. Harmony was used to integrate multiple data sets and eliminate the batch effect. Then the cell clustering and annotation were performed after data quality control. The data sets of the sorted vessel cells were not included in the analysis when calculating and comparing cell type ratios. However, those sorted data sets were included when performing cell function, cell-cell interaction analyses, etc. Ctrl indicates control.

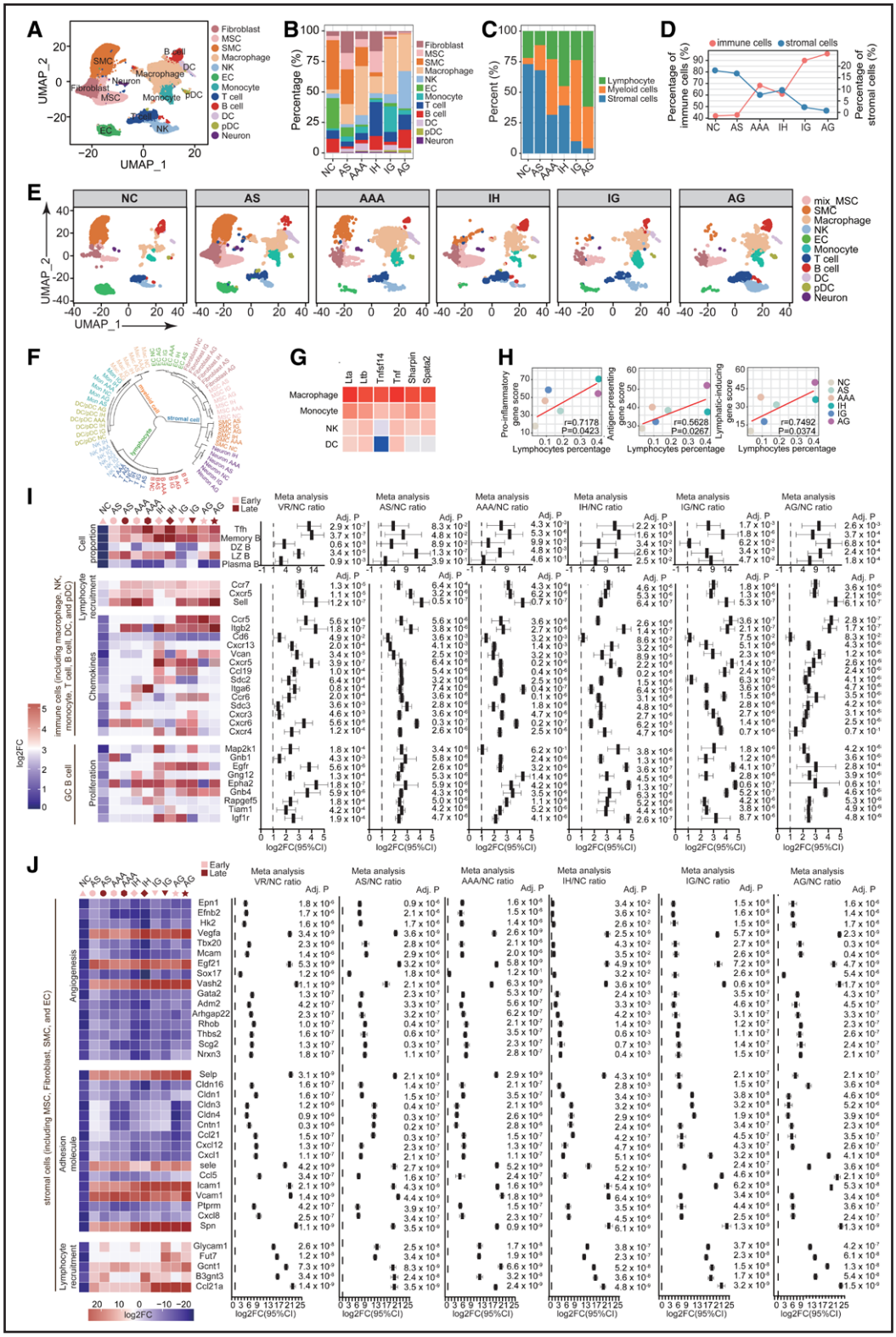

Figure 2. Chronic inflammation in the pathogenesis of vascular remodelings.

A, Uniform Manifold Approximation and Projection (UMAP) plot showing the major cell types in healthy and remodeled arteries. **B**, Bar graphs displaying the proportion of each cell type in total artery cells in the indicated groups as determined by single-cell RNA sequencing (scRNA-seq). **C**, Bar graphs displaying the proportions of lymphocytes (green), myeloid cells (orange), and stromal cells (blue) in total artery cells in the indicated groups as determined by scRNA-seq. **D**, Line graphs comparing the proportions of stromal cells and immune cells in total artery cells in the healthy and remodeled arteries as determined by scRNA-seq. **E**, UMAP plots showing cell types in normal control (NC) arteries and the atherosclerosis (AS), abdominal aortic aneurysm (AAA), intimal hyperplasia (IH), isograft (IG), and allograft (AG) models. **F**, (*Continued*)

Arterioscler Thromb Vasc Biol. 2023;43:1867–1886. DOI: 10.1161/ATVBAHA.123.318762

was used to perform enrichment analyses of Gene Ontology Biological Processes (Gene Ontology Biological Processes releases/2020-12-15 in g:Profiler) using differentially expressed genes expressed by selected cell clusters, and the data were visualized using the ggplot2 (version 3.4.2) package in R. *P* values were calculated based on a Wilcoxon rank-sum test. *P* value adjustment is performed using Bonferroni correction based on the total number of genes in the data set.

Visualization by Heatmap

The top differentially expressed genes between cell types were identified and combined between each data set. Average expression values for these genes or gene sets were then normalized by subtracting the mean expression and dividing by the SD of a given gene over all cells. Heatmaps were constructed based on these values; identified genes are shown as rows, whereas cells are shown as columns. Cells are grouped based on cell type, whereas genes are grouped based on specific gene sets or differential expression in the cell type from which they were identified. All these heatmaps and complete-linkage clustering showing correlation analyses were plotted using the R package pheatmap.

Cell-Cell Communication Analysis

We performed analyses of ligand-receptor pairs between cell types with the R package CellChat according to a previously described procedure.[21,27] We followed the official workflow: briefly, we loaded the normalized counts into CellChat and applied the standard preprocessing steps, including the functions identifyOverExpressedGenes, identifyOverExpressedInteractions, and projectData with a standard parameter set. Specific TLS-related precompiled mouse ligand-receptor interactions were selectively used as a priori network information (Table S5). We then calculated the potential ligand-receptor interactions between cells based on the functions computeCommunProb, computeCommunProbPathway, and aggregateNet using standard parameters.

Mouse-Human Integrated Analysis

We used the Seurat alignment procedure to do the mouse-human integrated analysis for Figure S5, which is designed to integrate scRNA-seq data across distinct data sets.[28] The following are the main steps comprising a typical workflow:

1. Convert mouse genes to human genes and gene selection.
2. Canonical correlation analysis and define a shared correlation space.
3. Identify rare nonoverlapping subpopulations.
4. Dynamic time warping for aligning correlated subspaces.
5. Integrated analysis of mice-human integrated data.

Search Strategy and Pathological Evidence Criteria

We conducted a systematic search of the literature in January 2022 by searching Medline, Embase, PubMed, and Web of Science from inception to January 2022. The MeSH search terms included the following: atherosclerosis, aneurysm, hyperplasia, isograft, and allograft. No language restrictions were applied. The included studies were not limited by species. Our search strategy was tailored to each database. The details of the search strategy are shown in the Supplemental Material. We then collected all hematoxylin and eosin–stained pathological figures in the included studies for the detection of TLSs in vascular remodeling.

Histology, Immunofluorescence Staining, Scanning, and Analysis

Briefly, 4 to 6 μm sections of remodeled vascular tissues were prepared and stained with hemotoxylin and eosin (IH in Figure S5A) or immunofluorescent antibodies (Figure 6). Hemotoxylin and eosin–stained sections were imaged using an Olympus DP71 camera. Sections from each mouse were visualized to be analyzed by a blinded observer with certified 3DHistech CaseViewer Software (version 2.3.0; Sysmex, Budapest, Hungary).

The antibodies used for immunofluorescence staining included fluorescein isothiocyanate (FITC)–anti-B220 (11-0460-82; eBioscience, San Diego, CA), rabbit anti-CD3 (ab16669; Abcam, Cambridge, MA), mouse anti-CD31 (910003; BioLegend, San Diego, CA), rat anti-MECA-79 (120801; BioLegend, San Diego, CA), rat anti-CD20 (ab27930; Abcam, Cambridge, MA), Cyanine3 donkey anti-rabbit IgG (406402; BioLegend, San Diego, CA), AF647 goat anti-rat IgG (405416; BioLegend, San Diego, CA), and FITC goat anti-mouse IgG (ab6785; Abcam, Cambridge, MA). After the fixed and blocked sections were incubated in primary antibodies for 3 hours at room temperature, the sections were washed twice with PBS and incubated with the appropriate fluorescent secondary antibodies for 1 hour. The nuclei were labeled with DAPI (236276; Roche, Basel, Switzerland).

Figure 2 Continued. Hierarchical clustering of major cell lineages. **G**, Heatmap (column scaled) showing the average gene expression levels in the indicated cells. **H**, Scatterplot showing the Pearson correlation coefficients between the proportions of lymphocytes in the late stage (divided by the total cells) and the expression scores of proinflammatory (**left**), antigen presentating–related (**middle**), and lymphatic-inducing (**right**) genes for innate immune cells in the indicated groups. **I**, Heatmap and forest plot comparing the cell proportions and expression levels of lymphocyte recruitment-, chemokine-, and cell proliferation–related genes in the indicated cells of remodeled vessels with those of healthy arteries. Cell types or previously published biomarkers are shown as rows, and individual scRNA-seq data sets are shown as columns. The heatmap indicates the proportion of a specific cell type or the effect size of a given gene marker in each data set (measured as the log2 odds ratio [OR] for the cell proportion and as the average gene expression in the indicated data sets vs the cell proportion or the average gene expression in the control group (NC) derived from logistic regression). The right-hand forest plot shows the overall effect size and significance of each marker in the meta-analysis across all studies based on effect sizes and SEs. The *P* values shown are derived from meta-analysis (random effects analysis because of the different vascular remodeling types). **J**, Heatmap and forest plot comparing the expression of angiogenesis-related, adhesion molecule–related, and lymphocyte recruitment–related genes in all stromal cells between remodeled vessels and healthy arteries. Adj P indicates adjusted *P* value; DC, dendritic cell; DZB, dark zone B cell; EC, endothelial cell; FC, fold change; LZB, light zone B cell; MSC, mesenchymal stem cell; NK, natural killer cell; pDC, plasmacytoid dendritic cell; SMC, smooth muscle cell; and VR, vascular remodeling.

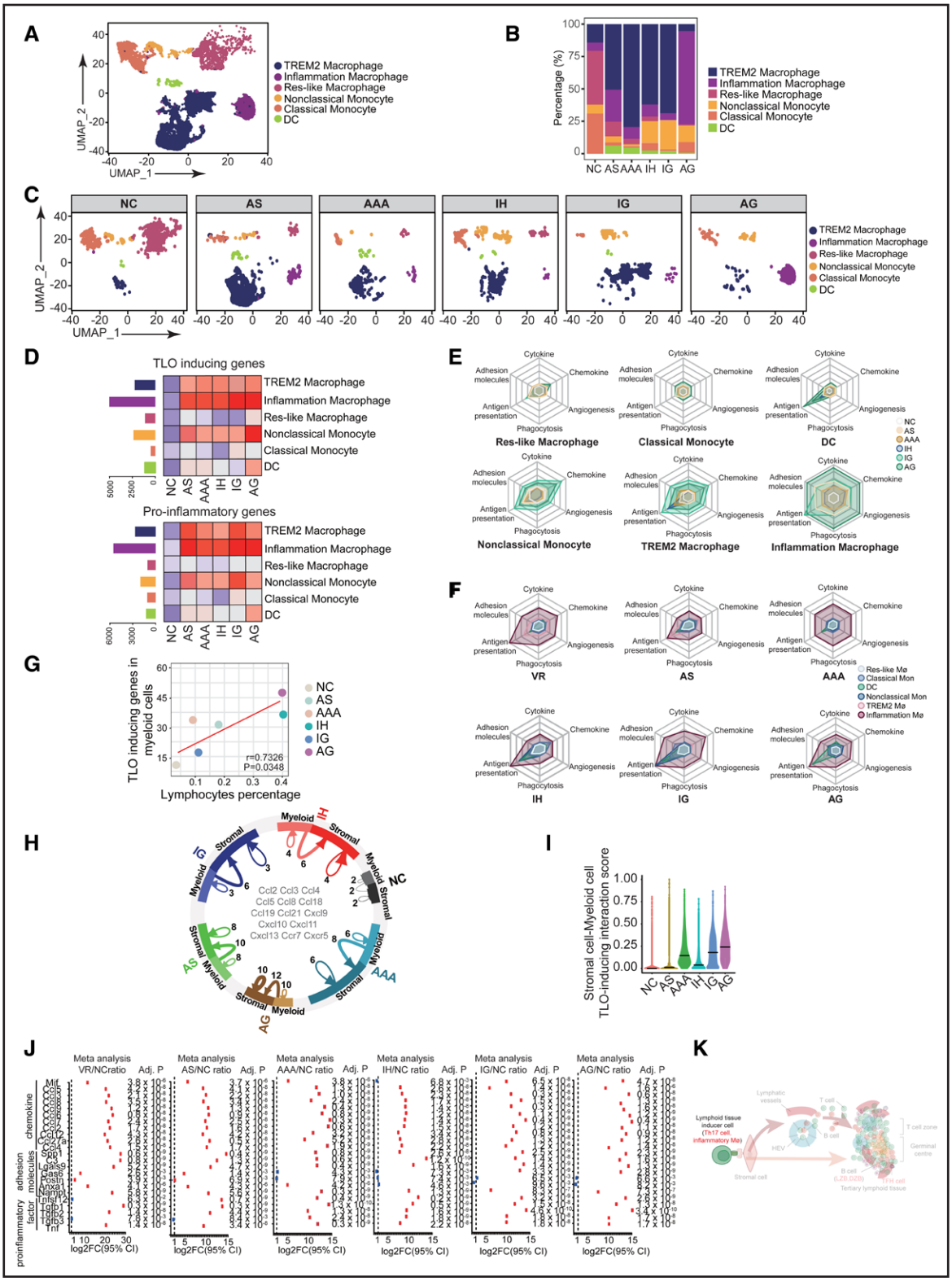

Figure 3. Myeloid cell population and transcriptional signaling for developing tertiary lymphoid organs (TLOs).
A, Uniform Manifold Approximation and Projection (UMAP) plot showing the myeloid cell subtypes in healthy and remodeled arteries. **B**, Bar charts displaying the proportion of each myeloid cell subtype in overall artery cells of the indicated groups by single-cell RNA sequencing (scRNA-seq). **C**, UMAP plots showing the myeloid cell subtypes in normal control (NC) artery, atherosclerosis (AS), abdominal aortic aneurysm (AAA), intimal hyperplasia (IH), isograft (IG), and allograft (AG). **D**, Heatmap showing the average gene expression of TLO-inducing genes (up) and proinflammatory genes (bottom) in the indicated cell subtypes (row) and groups (column). **E**, Gene expression signature of cytokine, chemokine, angiogenesis, phagocytosis, antigen-presenting, and adhesion molecule for specific myeloid cell subtypes of healthy and remodeled arteries; average gene expression for the reference is normalized between 0 and 1. **F**, Gene expression signature of (*Continued*)

Inclusion and Exclusion for Human Data Sets

Inclusion Criteria

Database: Gene Expression Omnibus database.
MeSH terms: atherosclerosis, aneurysm, hyperplasia, isograft, and allograft.
Species: *Homo sapiens*.
Dates: from inception to November 2022.

Excluded Studies That Met the Following Criteria

We only collected scRNA sequencing data, and the bulk RNA sequencing and sn-RNA sequencing data were excluded.

Statistical Methods

Log2(fold change) was used to compare differences between 2 studies based on scRNA-seq count data. The expression levels of target genes in each group were normalized to the reference group and presented as log2-transformed fold change. The 95% CIs were calculated using *Z* scores and SEs, while the *P* values were computed based on log2(fold change) and SE by *Z* test, resulting in 1-tailed *P* values. *P* value adjustment is performed by Benjamini-Hochberg. Statistical analysis was performed using R4.2.2 (http://www.r-project.org/). We considered a *P* value of 0.05 to be statistically significant.

RESULTS

Chronic Inflammation in the Pathogenesis of Vascular Remodeling

The workflow for the collection of data sets with interest is summarized in Figure 1A and 1B. Accumulating evidence has shown that inflammation plays a central role in the progression of various forms of vascular remodeling and leads to adverse cardiovascular events.[29] There have been great advances in the understanding of cellular and molecular mechanisms and their variations in these vascular pathologies due to the applications of single-cell technologies. Marker genes for cell cluster annotation have been well established in previous publications (Figure S1A through S1D; Table S1).[21,30] In healthy arteries, immune cells, including macrophages, T cells, B cells, and, to a lesser extent, DCs, form a small part of the resident cell population (Figure 2A through 2E).[31,32] Accumulation and infiltration of immune cells have been observed in various remodeling vessels, including atherosclerosis, AAA, IH, isograft, and allograft arteries (Figure 2A through 2E). Interestingly, the proportion of immune cells, including myeloid cells and lymphocytes, incrementally increases from atherosclerosis to IH, AAA, isograft, and allograft, whereas the proportion of stromal cells decreases significantly (Figure 2C and 2D). It is noteworthy that inflammatory responses are highly activated in graft arteries, with over 90% of vascular cells being immune cells (Figure 2C and 2D). Compared with the isograft model, the allograft model presents a higher adaptive immune response (Figure 2C and 2D). The proportion of B cells in healthy artery is ≈13%. B cells account for 3% to 5% of atherosclerosis, AAA, and isograft remodeling vessels, whereas ≈16% of IH and allograft remodeling vessels (Figure 2B and 2E). It is observed that smooth muscle cells (SMCs) gradually disappeared in the allograft vascular remodeling model via immunofluorescence staining, while the proportion of macrophages increased significantly (Figure S2A) and gradually infiltrated from the adventitia to the media (Figure S2B). The endothelial cells (ECs) in the normal control aorta include vascular ECs and <3% lymphatic ECs. However, the proportion of high endothelial venule ECs and lymphatic ECs increased in remodeled vessels (Figure S2C and S2D). To identify the functional similarities and differences in similar cell types among different models, we assessed similarities in the average transcriptome between each major lineage in different vascular remodeling models via cluster analysis (Figure 2F). As expected, similar cell lineages from vascular models clustered together but maintained differences at the transcriptional level among vascular models. This result indicates that the pathological mechanisms mediated by similar cell types are not entirely identical in different models (Figure 2F). Due to the close interplay between inflammation and vascular pathology, the heterogeneity of immune responses, as revealed by differences in immune cell numbers and transcriptional patterns, may determine the progression of various types of vascular remodeling.[29,33]

The first set of responses are innate immune responses in various vascular pathologies.[34] As demonstrated in our

Figure 3 Continued. cytokine, chemokine, angiogenesis, phagocytosis, antigen-presenting, and adhesion molecule of the specific myeloid models in different myeloid cell subtypes; average gene expression for the reference is normalized between 0 and 1. **G**, Scatterplot showing the Pearson correlation coefficients between the proportions of lymphocytes in the late stage (divided by the total cells) and the expression scores of TLO-inducing genes for myeloid cells in the indicated groups. **H**, Cellular interaction pairs between myeloid cells and stromal cells in the indicated models. The direction of the arrow represents the direction of cellular interaction, starting from the ligand cell and ending in the recipient cell. The numbers represent the number of ligand-receptor pairs. **I**, Violin plot showing the expression level for the related genes of ligand-receptor pairs between myeloid cells and stromal cells in the indicated models. **J**, Forest plot showing the overall effect size and significance of each marker in meta-analysis across all studies, based on effect sizes and SEs. *P* values are shown from meta-analysis (random effects, on account of the different vascular remodeling types). **K**, Schematic diagram showing the role of myeloid cells in the formation of TLO. Adj P indicates adjusted *P* value; CCL, chemokine (C-C motif) ligand; CXCL, chemokine (C-X-C motif) ligand; DC, dendritic cell; DZB, dark zone B cell; HEV, high endothelial venule; Lamp3, lysosomal-associated membrane protein 3; LZB, light zone B cell; Res-like, resident-like; Scl1, scarecrow-like protein 1; Tfh, follicular helper T-cell; Th, T helper; TREM2, triggering receptor expressed on myeloid cells 2; and VR, vascular remodeling.

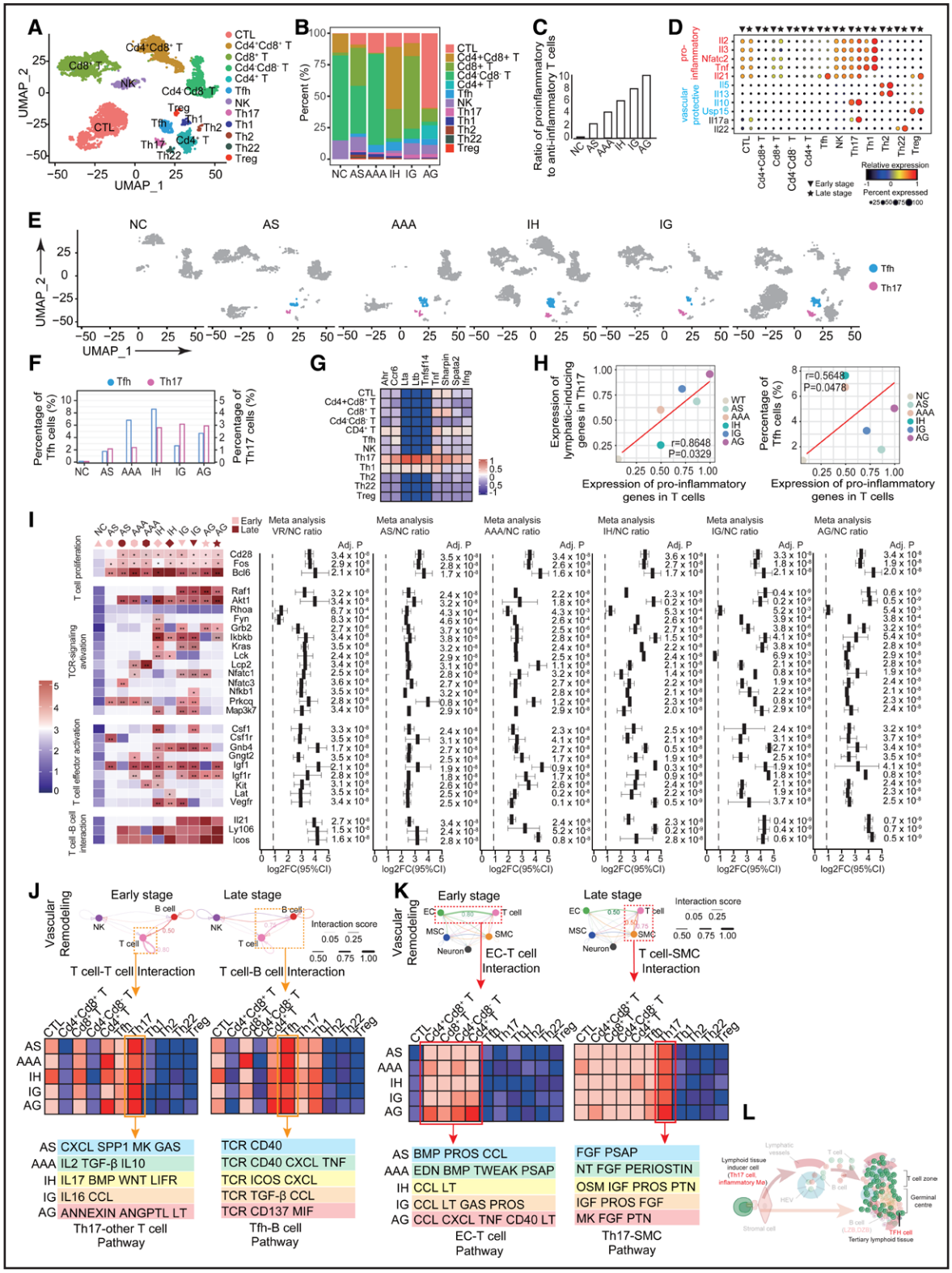

Figure 4. T lymphocytes and transcriptional signaling for developing tertiary lymphoid organs (TLOs).
A, Uniform Manifold Approximation and Projection (UMAP) plot showing the T-cell subtypes in healthy and remodeled arteries. **B**, Bar charts displaying the proportion of each T-cell subtype in overall T cells of the indicated groups by single-cell RNA sequencing (scRNA-seq). **C**, Bar charts displaying the ratio of proinflammatory to anti-inflammatory T cells of the indicated groups by scRNA-seq. **D**, Dot plots showing the expression of cytokine-related genes in each subset at early or late stage of vascular remodeling. **E**, UMAP plots showing follicular helper T cells (Tfh; blue) and T helper 17 (Th17; purple) in normal control (NC) artery, atherosclerosis (AS), abdominal aortic aneurysm (AAA), intimal hyperplasia (IH), isograft (IG), and allograft (AG). **F**, Bar charts displaying the proportion of Tfh (blue) and Th17 (purple) in total T (*Continued*)

results, compared with those in healthy vessels, the proportions of innate immune cells, including macrophages, monocytes, and DCs, were significantly increased at the early stage in the atherosclerosis, IH, AAA, isograft, and allograft models (Figure S1E and S1F). This innate immune response progressed to the chronic phase of vascular remodeling. The proportions of infiltrated macrophages and monocytes were also higher in vascular pathology models than in healthy vessels at the late stage of vascular injury (Figure S1E and S1F). A scaled proinflammatory gene score considering 92 genes was used to evaluate the proinflammatory activity of innate immune cells (Table S2). The overall proinflammatory gene scores were higher in the early phase of each type of vascular remodeling than in the later phase (Figure S1G). Innate immune cells induce an acute inflammatory response via their capability to produce chemokines, cytokines, lymphatic molecules, and MHC molecules with different antigen presentation capabilities to attract and activate T and B lymphocytes (Figure S1G). More importantly, among innate immune cells, macrophages secrete the highest amount of lymphoid cell–inducing molecules, for example, LT, LTβ, and the cytokine TNF (tumor necrosis factor), to play a role as lymphoid tissue inducer (LTi) cells and induce the formation of TLOs (Figure 2G).[35] Notably, the proinflammatory, antigen-presenting, and lymphatic genes expressed by innate immune cells in the early phase of vascular remodeling were positively correlated with the degree of lymphocyte infiltration in the late stage (Figure 2H).

In the integrated scRNA-seq data sets, we observed that structural cells of TLOs, including Tfh cells, memory B cells, GC B cells (dark zone [DZ] B and light zone [LZ] B cells), and plasma B cells, existed and were significantly increased in the remodeled vessels (Figure 2I). Notably, there were higher proportions of TLO structural cells in the allograft model than in other vascular injury models, which indicated that the allograft model may have an increased number of TLOs. The expression of transcriptional signaling molecules facilitating TLO formation among immune cells (including macrophage, natural killer, monocyte, T cells, B cells, DC, and plasmacytoid dendritic cell), including those facilitating lymphocyte recruitment (Ccr7, Cxcr5, and Sell)[35,36] and chemoattractants (Ccr5, Cxcr6, and Itgb2)[36] in all immune cells, and cell proliferation (Egfr, Epha2, Gnb4, and Igf1r)[36] in GC B cells was significantly upregulated in immune cells from vascular remodeling tissues (Figure 2I). In addition, the stromal cell population also plays an essential role in promoting TLO formation. Stromal cells produce angiogenetic signaling molecules (Vegfa, Egf21, and Vash2) facilitating high endothelial venule network formation and providing channels for lymphocyte mobilization to the perivascular zone. The production of adhesion molecules (Selp, Sele, Icam1, and Vcam1)[36,37] and lymphocyte recruitment molecules (Glycam1, Fut7, Gcnt1, B3gnt3, and Ccl21a)[36,37] by stromal cells (including mesenchymal stem cell, fibroblast, SMC, and EC)[37] attracts lymphocytes to migrate along chemokine gradients to the inflamed vascular site (Figure 2J; Figure S1I through S1K).

Our study highlights the involvement of innate and adaptive immunity in TLO formation in different vascular remodeling models. Notably, TLO structural cells were found in all remodeled vascular tissues and had enhanced transcriptional signaling related to TLO formation. In the following sections, we provide evidence showing the existence of TLOs in remodeled vasculature and highlight the signaling networks that support the generation of TLOs in specific cell populations.

Myeloid Cell Populations and Transcriptional Signaling in the Development of TLOs

A wide range of myeloid cells, including macrophages, DCs, monocytes, and neutrophils, are related to the progression of vascular remodeling.[38] In healthy arteries, myeloid cells are rare (7.13%). However, these cells permissively invade vessels beginning in the early stage of

Figure 4 Continued. cells of the indicated groups. **G**, Heatmap showing the expression of lymphatic tissue–inducing genes (column) in the indicated T-cell subtypes (row). **H**, Scatterplot showing the Pearson correlation of the gene expression of proinflammatory genes in T cells with lymphatic-inducing gene expression in Th17 (**left**) and the percentage of Tfh cell (**right**) by the indicated groups. **I**, Heatmap and forest plot comparing the expression of T-cell proliferation, TCR (T-cell receptor)-signaling activation, T-cell activation, and T-cell–B cell interaction-related genes in T cells of remodeled vessels with healthy arteries. **J**, Schematic diagram showing the interaction among T cell, B cell, and natural killer (NK) cell, and heatmap showing the interaction score of T cell–T cell and T cell B cell in the indicated groups (row) and T-cell subtypes (column) at the early and late stages of vascular remodeling. Top pathways are listed for the interaction of Th17 cell–other T-cell and Tfh–B cell. Statistical information corresponding to scores >0.25 was displayed. **K**, Schematic diagram showing the interaction among T cells, endothelial cell (EC), smooth muscle cell (SMC), mesenchymal stem cell (MSC), and neuron and heatmap showing the interaction score of EC–T-cell and T-cell–SMC in the indicated groups (row) and T-cell subtypes (column) at the early and late stages of vascular remodeling (**right**). Top pathways are listed for the interaction of EC–T cell and Th17-SMC. Statistical information corresponding to scores >0.25 was displayed. **L**, Schematic diagram showing the role of T cells in the formation of TLO. ANGPTL indicates angiopoietin-like protein; ANNEXIN, annexin; BMP, bone morphogenetic protein; CCL, C-C motif chemokine ligand; CXCL, C-X-C motif ligand; DZB, dark zone B cell; FGF, fibroblast growth factor; GAS, growth arrest-specific; ICOS, inducible costimulator; IGF, insulin growth factor; IL, interleukin; LIFR, leukemia inhibitory factor receptor; LT lymphotoxin; LZB, light zone B cell; MIF, macrophage migration inhibitory factor; MK, mitogen-activated protein kinase; NT, neurotrophin; OSM, oncostatin M; PERIOSTIN, periostin; PROS, protein S; PSAP, prostatic serum acid phosphatase; PTN, pleiotrophin; SPP1, secreted phosphoprotein 1; TGF-β, transforming growth factor-β; Treg, regulator T cell; VR, vascular remodeling; and WNT, wingless-type MMTV integration site family.

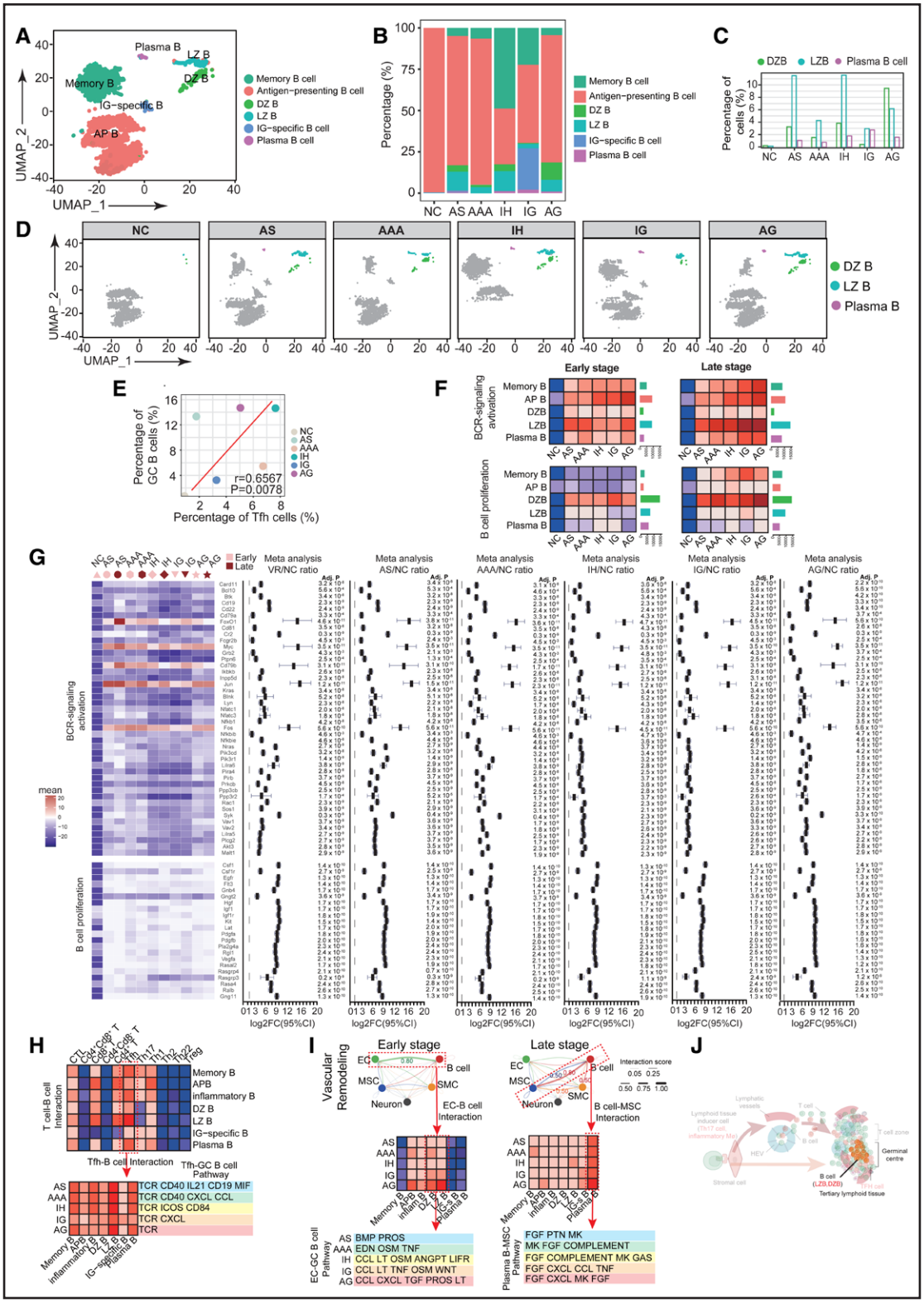

Figure 5. B lymphocytes and transcriptional signaling for developing tertiary lymphoid organs (TLOs).
A, Uniform Manifold Approximation and Projection (UMAP) plot showing the B-cell subtypes in healthy and remodeled arteries. **B**, Bar charts displaying the proportion of each B cell subtype in total B cells of the indicated groups by single-cell RNA sequencing (scRNA-seq). **C**, Bar charts displaying the proportion of dark zone B (DZ B; green), light zone B (LZ B; cyan), and plasma B (purple) cell in overall B cells of the indicated groups. **D**, UMAP plots showing DZ B (green), LZ B (cyan), and plasma B (purple) cell in normal control (NC) artery, atherosclerosis (AS), abdominal aortic aneurysm (AAA), intimal hyperplasia (IH), isograft (IG), and allograft (AG). **E**, Scatterplot showing the Pearson correlation of the percentage of follicular helper T cells (Tfh) with the percentage of germinal center (GC) B cells by the indicated groups. **F**, Heatmap showing the expression of BCR (B-cell receptor)-signaling activation and B-cell proliferation–related genes in the indicated (*Continued*)

Arterioscler Thromb Vasc Biol. 2023;43:1867–1886. DOI: 10.1161/ATVBAHA.123.318762

vascular injury (Figure S1E and S1F). The Seurat clustering algorithm implemented in Harmony clearly identified 6 subsets of myeloid cells in mouse vessels using well-demonstrated markers from previous publications (Figure S3A through S3E; Table S3).[39] We identified 2 monocyte subsets (including classical and nonclassical monocytes), 3 macrophage subsets (including resident-like macrophages, TREM2 macrophages, and inflammatory macrophages), and 1 DC subset (myeloid DCs).

In healthy vessels, resident-like macrophages accounted for the highest proportion (40.21%) of myeloid cells. However, in remodeled vessels, TREM2 macrophages and inflammatory macrophages were the most predominant myeloid cells and had the highest inflammatory score (Figure 3A through 3D; Figure S3F; Table S4). TREM2 macrophages had a similar gene expression profile that partially overlapped with that of inflammatory macrophages but highly expressed Trem2 (Figure 3A through 3C). Gene Ontology analysis assigned the TREM2 macrophages putative functions in lipid metabolism, cholesterol efflux, and lysosome function (Figure S3G). Inflammatory macrophages showed an even stronger proinflammatory gene profile and highly expressed TLO-inducing genes (eg, *Lta*, *Ltb*, *Tnfsf14*, and *Tnf*; Figure 3D; Figure S3G and S3H; Table S4). When comparing similar myeloid subclusters between different models, the expression levels of genes related to the characteristic functions of myeloid cells, including genes related to cytokines, chemokines, adhesion molecules, antigen presentation, angiogenesis, and phagocytosis, varied by model (Table S2). For instance, inflammatory macrophages, TREM2 macrophages, DCs, and classical and nonclassical monocytes had the highest expression of genes related to cytokines, chemokines, adhesion molecules, antigen presentation, angiogenesis and phagocytosis in the allograft model, followed by the isograft model (Figure 3E and 3F). Although inflammatory macrophages had the highest expression of genes related to cytokines, chemokines, adhesion molecules, antigen presentation, angiogenesis, and phagocytosis compared with the other myeloid cells, the weight of the signatures also varied by model. Inflammatory macrophages had more features related to antigen presentation than other features in the atherosclerosis, IH, isograft, and allograft models (Figure 3E and 3F). DCs were found to mainly function as antigen-presenting cells in the IH, isograft, and allograft models (Figure 3E and 3F) and actively interacted with lymphocytes, especially in the late stages of vascular remodeling (Figure S3I). We failed to identify sufficient neutrophils for analysis in the integrated data set, as was reported in the original publications.[40–42]

The generation of TLOs has similarities with secondary lymphoid organ formation.[43] Local production of chemokines by lymphocytes or stromal cells recruit LTi cells to the site of inflammation.[36] These LTi cells interact with local stromal cells, comparable to lymphoid tissue organizer cells in secondary lymphoid organs, particularly through LTα1β2 and LTβR (LTβ receptor) binding.[43] Inflammatory macrophages[44] have been shown to function as a substitute for LTi cells at the beginning of TLO generation in various pathological diseases and in vascular remodeling (Figure S3I). Among the recruited myeloid cell subtypes, macrophages, especially inflammatory macrophages, act as the predominant LTi cells during vascular remodeling-related lymphoid neogenesis because they express the highest levels of LT-related genes (eg, *Lta*, *Ltb*, and *Tnfsf14*; Figure 3D; Figure S3H). The allograft model presented the highest LT-related gene expression in myeloid cells (Figure S3J). This result explains why the allograft model has the highest proportion of lymphocytes. The results underscore the essential role of myeloid cells in TLO formation and vascular remodeling. In addition, TREM2 macrophages were also found to closely interact with stromal cells and highly express TLO-inducing chemokines and LT-related genes (Figure 3D; Figure S3I and S3J). Furthermore, we found that the expression levels of TLO-inducing chemokines in myeloid cell subtypes were proportional to those of proinflammatory genes (Figure 3D). Notably, the TLO-inducing genes in myeloid cell subtypes expressed by myeloid cells in the early phase of vascular remodeling were positively correlated with the degree of lymphocyte infiltration in the late stage (Figure 3G). In addition, DCs showed strong interactions with lymphocytes, especially in the late stage of vascular remodeling (Figure S3I).

Figure 5 Continued. B-cell subtypes (row) and groups (column) at the early (**left**) or late (**right**) stage during vascular remodeling (VR). **G**, Heatmap and forest plot comparing the expression of BCR signaling activation and B-cell proliferation–related genes in B cells of remodeled vessels with healthy arteries. **H**, The upper heatmap showing the interaction score of T cell–B cell in the indicated B-cell subtypes (row) and T-cell subtypes (column). The **bottom** heatmap showing the interaction score of Tfh–B cell in the indicated groups (row) and B cell subtypes (column). Top pathways are listed for the interaction of Tfh cell–GC B cell. **I**, Schematic diagram showing the interaction among B cells, endothelial cell (EC), smooth muscle cell (SMC), MSC, and neuron and heatmap showing the interaction score of EC–B cell and B cell–MSC in the indicated groups (row) and B cell subtypes (column) at the early and late stages of VR. Top pathways are listed for the interaction of EC–GC B cell and plasma B–MSC. Statistical information corresponding to scores >0.25 was displayed. **J**, Scatterplot showing the Pearson correlation of the percentage of Tfh cell with the percentage of germinal center B cell by the indicated groups. Adj P indicates adjusted *P* value; AP B, antigen-presenting B cell; BMP, bone morphogenetic protein; CCL, C-C motif chemokine ligand; CXCL, C-X-C motif ligand; DZB, dark zone B cell; ICOS, inducible costimulator; IL, interleukin; LIFR, leukemia inhibitory factor receptor; LT lymphotoxin; LZB, light zone B cell; MIF, macrophage migration inhibitory factor; MK, mitogen-activated protein kinases; OSM, oncostatin M; PROS, protein S; TCR, T-cell receptor; TGF-β, transforming growth factor-β; TNF, tumor necrosis factor; and WNT, wingless-type MMTV integration site family.

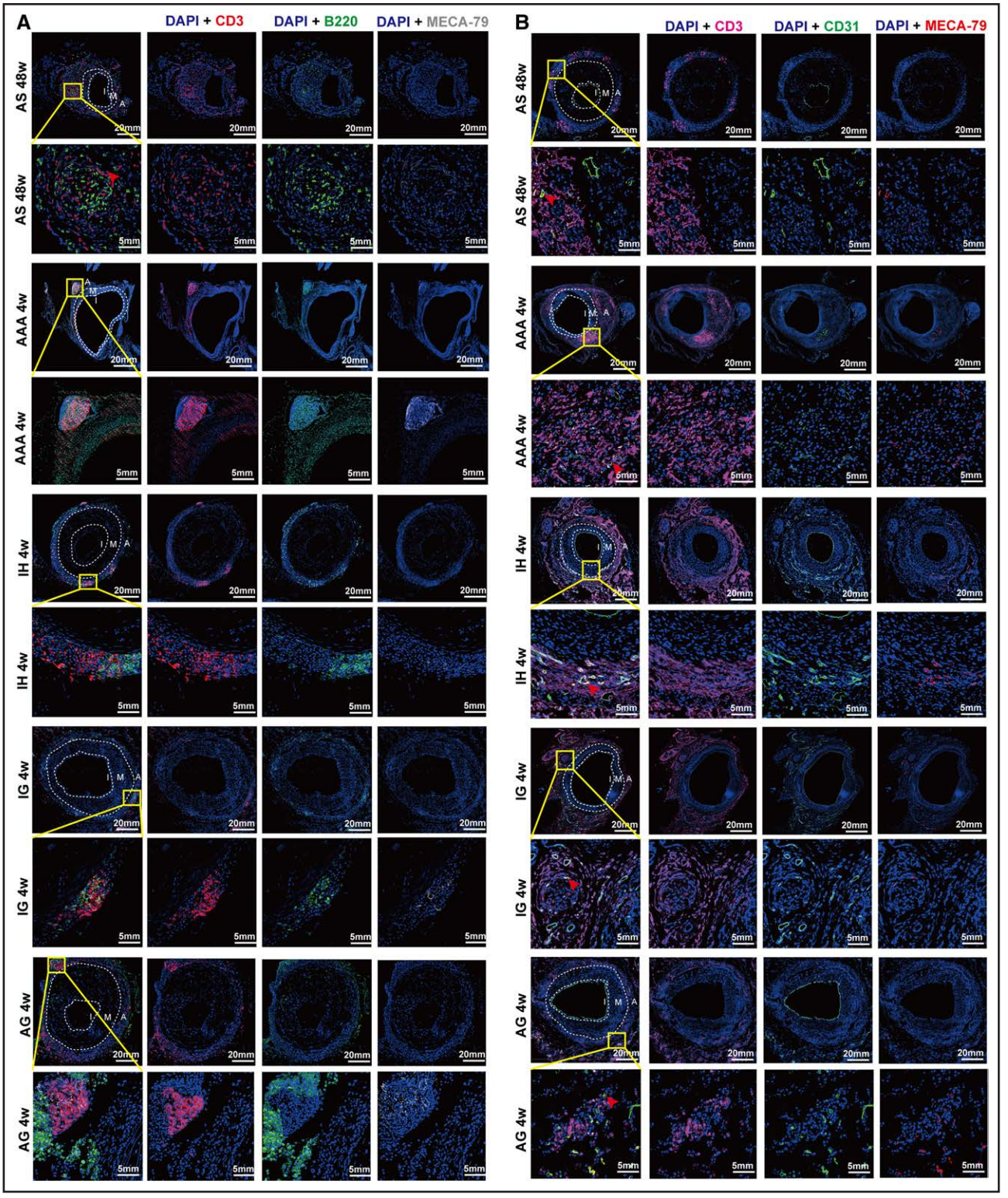

Figure 6. Immunofluorescence staining for vascular–tertiary lymphoid organs (TLOs).
A, Representative images showing T cells (CD [cluster of differentiation]3+, magenta), endothelial cells (CD31+, green), and high endothelial venule region (MECA-79+, red) enriched in TLO in the atherosclerosis (AS), intimal hyperplasia (IH), abdominal aortic aneurysm (AAA), isograft (IG), and allograft (AG) models. The **upper** part showing the overall structure and cell distribution of each type of remodeling vessel; higher magnifications are provided in the **lower** part. **B**, Representative images showing T cells (CD3+, magenta), endothelial cells (CD31+, green), and high endothelial venule region (MECA-79+, red) enriched in TLO in the AS, IH, AAA, IG, and AG models. The **upper** part showing the overall structure and cell distribution of each type of remodeling vessel; higher magnifications are provided in the **lower** part. A indicates adventitia; DAPI, 4',6-diamidino-2-phenylindole; I, intima; and M, media.

Using the integrated scRNA-seq data set, we also found that the myeloid cell population had the strongest interaction with vascular stromal cells, and this interaction was achieved via chemotaxis (Figure 3H; Figure S3I). The specific chemokines, such as CCL2 (C-C motif chemokine ligand 2) and CCL21, have been shown to be involved in TLO formation in previously published literature (Table S5).[36] There were 2 myeloid-stromal cell interaction pairs in normal arteries, 6 pairs in the IH model and isograft model, 8 pairs in the AAA model, 10 pairs in the atherosclerosis model, and 12 pairs in the allograft model (Figure 3H). The allograft model had the most myeloid-stromal cell interaction pairs (Figure 3I). Furthermore, the expression levels of chemokines, adhesion molecules, and proinflammatory factors in total myeloid cells were significantly higher in the models than in normal arteries, and the allograft model had the highest levels (Figure 3J).

In summary, myeloid cells not only initiate an acute inflammatory response during vascular injury but also act as LTi cells and antigen-presenting cells to attract and activate lymphocytes to form TLOs (Figure 3K).

T Lymphocytes and Transcriptional Signaling in the Development of TLOs

T cells are present both in healthy arteries and remodeled vessels but with a remarkably higher proportion and heterogeneity in remodeled vessels (Figure 4A and 4B).[31] The markers for identifying T-cell subclusters have been defined in previous publications (Figure S4A; Table S6).[21,45] The proportions of effector T cells, including Cd4$^+$ T cells, Cd8$^+$ T cells, cytotoxic T lymphocytes, Tfh cells, T helper (Th) 17 cells, Th1 cells, Th2 cells, Th22 cells, and regulator T cells, in total vascular cells were increased in the vascular remodeling models (Figure S4B). Th17 and TFH cells were also observed in human-remodeled vessels (Figure S5). Among effector T cells, proinflammatory T cells, including Th17, Th1, and Th22 cells, were more predominant than immune regulatory T cells, such as regulator T cells, in remodeled vessels (Figure 4A and 4B; Figure S4B). The proportions of proinflammatory to anti-inflammatory T cells were highest in the isograft, allograft, and IH models (Figure 4A through 4C; Table S7). These T cells secrete different levels of cytokines in the early and late stages of vascular remodeling (Figure 4D). Both proinflammatory factors (including IL [interleukin]-2, IL-3, TNF, and IL-21) and vascular protective factors (including IL-5, IL-13, IL-10, and TGF [transforming growth factor]-β) were found to be secreted by effector T cells, generally showing higher expression in the late stage than in the early stage (Figure 4D).[46]

Th17 cells have emerged as a new Cd4$^+$ T-cell subset that characteristically secrete IL-17A, IL-17F, IL-21, and IL-22 to contribute to proinflammatory responses in vascular injury.[47] Importantly, it has been reported that Th17 cells can function as a substitute for LTi cells in the initiation of lymphoid neogenesis in various pathological contexts.[48] From the normal control to the atherosclerosis, AAA, IH, isograft, and allograft models, the proportion of Th17 cells incrementally increased (Figure 4E and 4F). Moreover, the average expression of Th17-cell signature cytokine genes also increased in the same pattern (Figure S4C). As shown in Figure 4G, Th17 cells expressed the highest levels of surface LT heterotrimer and other lymphatic developmental factors, transcription factors, and cell surface markers, including AHR, CCR6, and LTs, among T-cell subtypes.[48] The lymphatic tissue–inducing capacity of Th17 cells varied by model. For instance, the expression of lymphatic tissue–inducing genes, such as *Lta*, *Ltb*, and *Sharpin*, was higher in all vascular remodeling tissues, with the highest expression in the allograft model, followed by the isograft model (Figure S4D).

Tfh cells are a specialized subset of Cd4$^+$ T cells that play a significant role in providing critical help for B-cell somatic hypermutation and maturation within the GCs of TLOs. Few Tfh cells were observed in healthy vessels, while the proportion of Tfh cells was markedly increased in remodeled vessels (Figure 4E and 4F). Furthermore, the proportions of Tfh-like cells marked with Bcl6, Irf3, and Irf7 but negative for CXCR5, as well as the expression of genes that promote Tfh cell differentiation (Figure S4F; Table S2), were also elevated in remodeled vessels.

A complex network of interactions between T lymphocytes and the vascular microenvironment exists in vascular remodeling and has crucial roles in the chronic immune responses that lead to the development of local lymphatic organs (Figure 4L).[49] Notably, the expression level of proinflammatory genes in T cells was found to be tightly associated with the expression of lymphatic genes in Th17 cells and the proportion of Tfh cells in different models (Figure 4H). Using the integrated scRNA-seq data set, we found that T-cell proliferation, TCR (T-cell receptor) signaling, T-cell effector activation, and T-cell–B-cell interactions were upregulated in all the vascular injury models (Figure 4I).

The interactions of T cells with other cell types within the milieu were found to be extraordinarily dynamic. In the early stage, T cells mainly interacted with T lymphocytes among all lymphocytes (Figure 4J; Figures S4G and S3H; Table S8) and interacted with ECs among stromal cells (Figure 4K; Figure S4I; Table S8). Notably, Th17 cells, as LTi cells, showed the strongest interaction with other vascular T lymphocytes during the early phase of vascular injury (Figure 4J; Table S8), whereas the T-cell with which Th17 cells interacted most strongly varied in different models (Figure 4J; Table S8). Furthermore, in the early phase, ECs attracted naive T cells (Cd4$^-$Cd8$^-$ and Cd4$^+$Cd8$^+$ T cells), and Cd4$^+$ and Cd8$^+$ T cells mainly relied on the CCL pathway during vascular remodeling (Figure 4K; Table S8).

In the late stage of vascular injury, the interaction between T and B lymphocytes was enhanced among all lymphocytes (Figure 4J; Figure S4G and S4H; Table S8). Furthermore, T cells had stronger interactions with stromal cells, particularly with SMCs (Figure S4I). Given that Tfh cells are critical for the development of GCs in TLOs, it is not surprising that B cells showed the highest interaction with Tfh cells (Figure 4J). Tfh cells were found to communicate with B cells mainly through TCR and costimulatory pathways in the models (Figure 4J; Table S8). In the later phase, the interaction between T cells and stromal cells increased (Figure S4G through S4I). The main interactions were between Th17 cells and SMCs (Figure 4K). However, the major mechanism mediating Th17-cell and SMC interactions differed among the models. For example, the predominant signaling pathways activated in the atherosclerosis model were the FGF (fibroblast growth factor) and PSAP (prostatic serum acid phosphatase) signaling pathways, while the MK (mitogen-activated protein kinases), FGF, and PTN (pleiotrophin) signaling pathways were activated in the allograft model (Figure 4K; Table S8).

B Lymphocytes and Transcriptional Signaling in the Development of TLOs

B lymphocytes are inflammatory cells that are recruited to remodeled vessels in response to various vascular injuries.[50,51] In normal arteries, there are very few B cells, and the majority of B-cell clusters contain antigen-presenting B cells. The quantity and complexity of B cells were increased in remodeled arteries, which were composed of memory B, antigen-presenting B, DZ B, LZ B, isograft-specific, and plasma B cells (Figure 5A and 5B; Figure S6A; Table S9).[21] Also, germinal center B cells were observed in human-remodeled vessels (Figure S5). A previous study reported that B cells are recruited to the vascular adventitia.[52] In addition to diffuse perivascular infiltrates, B cells come together with activated T cells and DCs to form organized local TLOs.[11] GC B cells, including LZ B and DZ B cells, and plasma cells are distinct B-cell populations present in TLOs, and these populations were largely increased in the indicated remodeled vessels (Figure 5C and 5D). The number of LZ B and DZ B cells was tightly associated with the quantity of Tfh cells in different models (Figure 5E). B cells, particularly LZ B cells, AP B cells, and memory B cells, showed upregulated expression of genes related to BCR (B-cell receptor) signaling promoting B-cell proliferation (Csf1, Efna5, Epha2, Fgf1, etc) and BCR gene rearrangement (Myc, FoxO1 [forkhead box O1], etc) in remodeled vessels compared with healthy vessels (Figure 5F and 5G). DZ B cells had the highest proliferative properties among B-cell populations in the vascular injury models (Figure 5F and 5G). Pathways related to the maintenance of TLOs showed higher activities in the later stage of vascular remodeling than in the early stage (Figure 5F and 5G).[53] Follicle B cells are one of the key cell types for TLO formation. Since the number of follicle B cells is limited, we failed to capture such B cells during single-cell sequencing. We further performed immunofluorescence staining evidence to confirm that the follicle B cells exist in TLOs of the remodeled vessels. Immunofluorescence imaging showed CD20 expressing B cells mainly resided in $CD3^+B220^+$ cells aggregated area (Figure S6F).

As shown in the ligand-receptor interaction analysis, B-cell subtypes had the closest interactions with T lymphocytes (Figure 4I; Figures S4H and S6B), especially with Tfh cells (Figure 5H), during vascular remodeling. LZ B cells were found to interact with Tfh cells mainly through TCR-associated pathways in the various remodeled vessel models (Figure 5H). The interactions between stromal cells and B cells were found to increase and play a more dominant role during the late phase of vascular remodeling (Figure S6B). Furthermore, there were differences in the interactions between B cells and stromal cell subtypes in different phases of vascular remodeling (Figure 5I; Figure S6C; Table S8). In the early stage, the interactions were the highest between GC B cells (LZ and DZ B cells) and ECs. In the later stage, plasma B-cell and mesenchymal stem cell interactions became dominant, and these interactions were primarily mediated by FGF pathways in the models (Figure 5I; Figure S6C; Table S8). In summary, B lymphocytes are involved in the development of TLOs and the active inflammatory response in the GC during vascular remodeling (Figure 5J).

In Situ and Human Evidence of TLO Generation in Vascular Remodeling

The above-mentioned RNA-seq data strongly supported that TLOs appear in remodeled vascular tissue. To obtain more direct evidence supporting the presence of TLOs in such vascular pathologies, we provide immunofluorescence staining and observed T cells ($CD3^+$) and B cells ($B220^+$) aggregated in para-vascular TLO. Meanwhile, high endothelial venule ($MECA\text{-}79^+$) colocalized with TLO in atherosclerosis, AAA, IH, isograft and allograft from

Table. Information of Published HE-Stained Images of TLOs in Vascular Remodeling Models

Model	Species	Reference	
AS	Mice	Isoda et al[72]	Figure 4A
AS	Human	Akhavanpoor et al[73]	Figure 3A
AS	Human	van Dijk et al[74]	Figure 4
AAA	Human	Roberts et al[75]	Figure 5
AAA	Human	Trinidad-Hernandez et al[76]	Figure 4
AG	Mice	Cai et al[77]	Figure 4I

AAA indicates abdominal aortic aneurysm; AG, allograft; AS, atherosclerosis; HE, hematoxylin and eosin; and TLO, tertiary lymphoid organs.

rodents (Figure 6A and 6B; Figure S7). Also, we systemically reviewed vascular remodeling studies and examined HE-stained images of the atherosclerosis, AAA, IH, isograft, and allograft from rodents and humans with these diseases and found organized and tight lymph node-like structures in the adventitia area of remodeled arteries, particularly on the sides with more severe IH (Table; Figure S8). Both in mice and in human data, we defined the key cell types for vascular TLO formation. The finding in human-remodeled vessels is consistent with the findings in mice (Figure S5; Tables S11 through S13).

DISCUSSION

We integrated 28 scRNA-seq data sets derived from 5 vascular remodeling model types to systematically explore the existence of TLOs and the complexity of the environment that supports their growth. The structural cells of TLOs and their inducing conditions, including myeloid cell populations, Tfh cells, Th17 cells, GC B cells, and stromal cells, were observed in all remodeled vessels. Notably, the levels of inflammatory responses in TLi cells varied among the models and were tightly associated with the numbers of TLO structural cells. We also systematically reviewed vascular remodeling studies and obtained direct evidence supporting the presence of TLOs using histological images. This study shows that TLOs are present in remodeled vessels and provides a resource to explore the mechanisms mediating TLO formation in vascular pathology.

TLOs are highly active lymphatic organs that develop in sites with long-lasting inflammatory responses, such as in tumor tissue and tissues in autoimmune diseases.[36] Our group was the first to identify vascular-associated lymphoid tissue surrounding atherosclerotic lesions approximately 3 decades ago.[17–19] Later studies also showed TLOs in the aorta adventitia adjacent to atherosclerotic plaques in Apoe$^{-/-}$ mice during aging, and the size of the TLOs was correlated with vascular remodeling severity in an LTβR-dependent manner.[54–56] The presence of TLOs is not limited to atherosclerosis and is also found in other vascular pathologies. Researchers have found that TLOs are involved in the development of aneurysms and that blocking proteasome-associated TLO formation significantly attenuates the development of aneurysms and allograft remodeling.[57,58] Recently, we also discovered the local formation of TLOs in allograft arteriosclerosis, which was found to be detrimental to the long-term survival of transplant tissues.[21] Based on such observations, we reasoned that the presence of TLOs could be a common phenomenon in remodeled vessels and may indicate therapeutic potential. Therefore, we leveraged scRNA-seq data sets from atherosclerosis, AA, IH, isograft, and allograft models to explore this hypothesis.

Our vascular scRNA-seq analysis showed that both the innate and adaptive immune systems participated in vascular remodeling in all the models, while the extent to which each immune system participated varied among the models. The models of transplant vascular pathologies, including the isograft and allograft models, demonstrated the strongest inflammatory response, followed by the AA and IH models. The atherosclerosis model had the lowest number of immune cells. In addition, the level of the inflammatory response, especially in the early phase of vascular injury, was closely associated with the numbers of TLO structural cells in the later phase. Interestingly, this finding is in agreement with the clinical observation that 50% of transplant vessels show graft arteriopathy within 5 years, which is the leading cause of restenosis in vascular pathology.[59,60] The rate of restenosis is as high as 51% in peripheral arterial intervention.[61] For atherosclerosis, narrowing of the diameter of the coronary artery (stenosis) by 50% takes 3 years or 5 years.[62] The correlation between the immune responses and clinical deterioration rates for each vascular pathology further supports the important role of the immune response in their progression.

Using longitudinal scRNA-seq data derived from vascular remodeling models, we analyzed the vascular microenvironment that serves as the soil for the seeding and proliferation of tertiary lymph nodes. Myeloid cells are one of the major cell types detected at an early stage of vascular remodeling and have the strongest interaction with stromal cells.[30] In our study, the myeloid cell population interacted with stromal cells via chemotactic effects related to CCLs and CCRs, which potentiate the recruitment of lymphocytes during vascular remodeling. We also demonstrated that among myeloid cells, inflammatory macrophages acted as the predominant LTi cells initiating TLO generation. A series of recent large-scale genetic and observational epidemiological studies and data from human atherosclerotic plaques highlight the relevance and therapeutic potential of the CCL2-CCR2 axis in human atherosclerosis.[63] In addition to inflammatory macrophages, Th17 cells are regarded as vital LTi cells. Th17 cells and cytokines, such as IL-17 and IL-22, contribute to the development of ectopic lymphoid structures in chronically inflamed tissue.[64] In our study, Th17 cells had the strongest interaction with other T cells beginning in early vascular injury. Such LTi cells seed the developing perivascular lymphoid organs in the vascular microenvironment and are essential for determining TLO formation and the degree of vascular remodeling.

LTi cells produce chemokines and cytokines that allow lymphatic cells, including T cells and B cells, to travel to perivascular spaces via high endothelial venules.[65] The presentation of self-antigens or allogenic antigens by DCs and education of subsequent T-cell and B-cell responses result in the generation of effector T cells and B cells and antibodies. Thus, it is not surprising that we observed strong interactions of T cells and B cells with ECs via CCL, CXCL (C-X-C motif ligand), and LT BMP (bone morphogenetic protein) pathway signaling in the

early phase of vascular injury. In the late phase of vascular injury, TCR, CD40 (cluster of differentiation 40), and CXCL signaling interactions between T cells and B cells became highly active, which potentiated T-cell and B-cell development and maturation. Among the T-cell population, Tfh cells are a specialized subset of $CD4^+$ T cells located in lymphoid organs and play a critical role in helping B cells in BCR recombination and antibody production to combat foreign pathogens. We observed a significant number of Tfh cells in all vascular injury models, and these cells showed strong interactions with B cells, particularly with LZ B cells. Recent studies have identified T-cell-dependent B cells as potent proatherogenic mediators in ApoE-knockout mouse models.[66,67] Restoring control of the Tfh-GC B-cell axis by blocking the inducible costimulator–ICOSL interaction reduced lesion development in atherosclerotic and artery-transplanted mice.[53,68] Notably, in our results, the inducible costimulator–ICOSL interaction in the IH model played a significant role in vascular remodeling, although this result needs to be further verified. Tfh cells select high-affinity B cells for clonal expansion in GCs,[69] we also observed markedly enhanced B cell proliferation and BCR signaling during vascular remodeling. The active T-B cell interactions and lymphocyte activation in GC response are crucial in the generation of efficacious immunity.[70] In healthy arteries, B cells are found in the adventitia and perivascular adipose tissue, with a higher proportion than some remodeling vessel.[31,71] It is due to large number of immune cells infiltrated in various remodeling vessels, which take up great propositions of cells in vessels. The actual number of B cells increased in remodeling vessels. Moreover, B cells in healthy vessel are antigen-presenting B cells rather than antibody-producing plasma B cells or highly activated germinal center B cells.[71]

Regarding study limitations, we acknowledge that the data set of our study was derived from data from a diverse set of previously published studies; however, the bioinformatics data processing was standardized. Although we find that different vessel parts had similar cellular composition and signature gene expressions, the impact of different vessel parts collected in atherosclerosis, aneurysm, and hyperplasia models on the results should not be neglected when comparing gene expression levels during functional analysis. No significant difference exists in cell clustering and average gene expressions of the data with different sequencing depths ranging from 40 000 to 908 007, but the potential bias from sequencing depth might still bring in unwanted bias. In addition, we estimated expression at the mRNA level rather than the protein level, especially some T-cell subsets, and thus, the results need to be further explored and verified. Moreover, due to limitations of the public databases, we only studied murine models of artery remodeling. Although several pathological images of human tissues were included in the study, the heterogeneity of TLO structures in human arteries deserves further research. Our studies both in mice and in human data define key cell types for vascular TLO formation. The finding in human-remodeled vessels is consistent with the findings in mice and provides a mechanistic basis and human context for further clinical translation targeting TLO for alleviating vascular remodeling.

In summary, we systematically explored the existence of TLOs and the microenvironment responsible for the growth of lymphatic organs in 5 vascular injury models. Mechanistically, myeloid cells interact with stromal cells via CCLs-CCRs potentiating the recruitment of lymphocytes. Along a chemokine gradient, T cells interact with TLi cells via CCLs, CXCLs, LT, and BMP to infiltrate. Although B cells mainly interact with T cells, particularly Tfh via TCR, CD40, and CXCLs for development and maturation in the germinal center. Our data can serve as a resource to gain a deeper understanding of the mechanisms mediating TLO formation in vascular pathologies and may provide valuable insights for new therapeutic strategies targeting various forms of vascular injury.

ARTICLE INFORMATION

Received February 10, 2023; accepted August 1, 2023.

Affiliations

Department of Cardiology (X.S., J.W., Q. Wen, Z.L., Y.T., Y.S., T.H., L.L., W.H., C.W., J.C.) and The Center of Clinical Pharmacology (Y.L., H.Y.), The Third Xiangya Hospital and High-Performance Computing Center (Q. Wu), Central South University, Changsha, China. Centre for Clinical Pharmacology, William Harvey Research Institute, Barts and The London School of Medicine and Dentistry, Queen Mary University of London, United Kingdom (Q. Xiao, Q. Xu). Department of Cardiology, The First Affiliated Hospital, School of Medicine, Zhejiang University, China (Q. Xu).

Acknowledgments

This work was also supported, in part, by the High-Performance Computing Center of Central South University. X. Sun, Y. Lu, and J. Wu analyzed and interpreted the single-cell RNA sequencing data, and wrote the initial draft. Q.W and Z. Li systematically searched and collected single-cell sequencing data sets and pathological images of vascular remodeling. Y. Tang, Y. Shi, and T. He constructed mice model of intimal hyperplasia, collected samples for single-cell RNA sequencing, and provided assistance in bioinformatics and statistical analysis. L. Liu performed single-cell RNA sequencing analysis, analyzed and curated data, and organized figures. W. Huang and C. Weng organized the figures and tables and checked the raw data. Q. Wu provided assistance for data integration and technical support for high-performance computers. Q. Xiao and H. Yuan provided data interpretation, constructive suggestions, and material support. Q. Xu and J. Cai conceived the idea, designed projects, performed critical reviews of the article, supervised the study and approved to publish, and provided funding for the study. All authors read and approved the article.

Sources of Funding

This work was supported by the National Natural Science Foundation of China 82170436 (J. Cai), Hunan Key Research and Development Project 2022SK2030 (J. Cai), the National Natural Science Foundation of China (81800393 [Y. Lu], 81770403 [H. Yuan], 82030008 [Q. Xu], and 81974054 [H. Yuan]).

Disclosures

None.

Supplemental Material

Systematic Review Searching Record
Tables S1–S13
Figures S1–S7
Major Resources Table

REFERENCES

1. Cui X, Pan G, Chen Y, Guo X, Liu T, Zhang J, Yang X, Cheng M, Gao H, Jiang F. The p53 pathway in vasculature revisited: a therapeutic target for pathological vascular remodeling? *Pharmacol Res*. 2021;169:105683. doi: 10.1016/j.phrs.2021.105683
2. Pethig K, Heublein B, Meliss RR, Haverich A. Volumetric remodeling of the proximal left coronary artery: early versus late after heart transplantation. *J Am Coll Cardiol*. 1999;34:197–203. doi: 10.1016/s0735-1097(99)00159-x
3. Galkina E, Ley K. Immune and inflammatory mechanisms of atherosclerosis (*). *Annu Rev Immunol*. 2009;27:165–197. doi: 10.1146/annurev.immunol.021908.132620
4. Weih F, Grabner R, Hu D, Beer M, Habenicht AJ. Control of dichotomic innate and adaptive immune responses by artery tertiary lymphoid organs in atherosclerosis. *Front Physiol*. 2012;3:226. doi: 10.3389/fphys.2012.00226
5. Gu W, Nowak WN, Xie Y, Le Bras A, Hu Y, Deng J, Issa Bhaloo S, Lu Y, Yuan H, Fidanis E, et al. Single-cell RNA-sequencing and metabolomics analyses reveal the contribution of perivascular adipose tissue stem cells to vascular remodeling. *Arterioscler Thromb Vasc Biol*. 2019;39:2049–2066. doi: 10.1161/ATVBAHA.119.312732
6. Cheng J, Gu W, Lan T, Deng J, Ni Z, Zhang Z, Hu Y, Sun X, Yang Y, Xu Q. Single-cell RNA sequencing reveals cell type- and artery type-specific vascular remodelling in male spontaneously hypertensive rats. *Cardiovasc Res*. 2021;117:1202–1216. doi: 10.1093/cvr/cvaa164
7. Gu W, Ni Z, Tan YQ, Deng J, Zhang SJ, Lv ZC, Wang XJ, Chen T, Zhang Z, Hu Y, et al. Adventitial cell atlas of wt (wild type) and ApoE (apolipoprotein E)-deficient mice defined by single-cell RNA sequencing. *Arterioscler Thromb Vasc Biol*. 2019;39:1055–1071. doi: 10.1161/ATVBAHA.119.312399
8. Jiang L, Sun X, Deng J, Hu Y, Xu Q. Different roles of stem/progenitor cells in vascular remodeling. *Antioxid Redox Signal*. 2021;35:192–203. doi: 10.1089/ars.2020.8199
9. Kokkinopoulos I, Wong MM, Potter CMF, Xie Y, Yu B, Warren DT, Nowak WN, Le Bras A, Ni Z, Zhou C, et al. Adventitial SCA-1(+) progenitor cell gene sequencing reveals the mechanisms of cell migration in response to hyperlipidemia. *Stem Cell Rep*. 2017;9:681–696. doi: 10.1016/j.stemcr.2017.06.011
10. Jiang L, Chen T, Sun S, Wang R, Deng J, Lyu L, Wu H, Yang M, Pu X, Du L, et al. Nonbone marrow CD34(+) cells are crucial for endothelial repair of injured artery. *Circ Res*. 2021;129:e146–e165. doi: 10.1161/CIRCRESAHA.121.319494
11. Mohanta SK, Yin C, Peng L, Srikakulapu P, Bontha V, Hu D, Weih F, Weber C, Gerdes N, Habenicht AJ. Artery tertiary lymphoid organs contribute to innate and adaptive immune responses in advanced mouse atherosclerosis. *Circ Res*. 2014;114:1772–1787. doi: 10.1161/CIRCRESAHA.114.301137
12. Neyt K, Perros F, GeurtsvanKessel CH, Hammad H, Lambrecht BN. Tertiary lymphoid organs in infection and autoimmunity. *Trends Immunol*. 2012;33:297–305. doi: 10.1016/j.it.2012.04.006
13. Fridman WH, Meylan M, Petitprez F, Sun CM, Italiano A, Sautes-Fridman C. B cells and tertiary lymphoid structures as determinants of tumour immune contexture and clinical outcome. *Nat Rev Clin Oncol*. 2022;19:441–457. doi: 10.1038/s41571-022-00619-z
14. Helmink BA, Reddy SM, Gao J, Zhang S, Basar R, Thakur R, Yizhak K, Sade-Feldman M, Blando J, Han G, et al. B cells and tertiary lymphoid structures promote immunotherapy response. *Nature*. 2020;577:549–555. doi: 10.1038/s41586-019-1922-8
15. Cabrita R, Lauss M, Sanna A, Donia M, Skaarup Larsen M, Mitra S, Johansson I, Phung B, Harbst K, Vallon-Christersson J, et al. Tertiary lymphoid structures improve immunotherapy and survival in melanoma. *Nature*. 2020;577:561–565. doi: 10.1038/s41586-019-1914-8
16. Jamaly S, Rakaee M, Abdi R, Tsokos GC, Fenton KA. Interplay of immune and kidney resident cells in the formation of tertiary lymphoid structures in lupus nephritis. *Autoimmun Rev*. 2021;20:102980. doi: 10.1016/j.autrev.2021.102980
17. Xu Q, Kleindienst R, Waitz W, Dietrich H, Wick G. Increased expression of heat shock protein 65 coincides with a population of infiltrating T lymphocytes in atherosclerotic lesions of rabbits specifically responding to heat shock protein 65. *J Clin Invest*. 1993;91:2693–2702. doi: 10.1172/JCI116508
18. Xu Q, Willeit J, Marosi M, Kleindienst R, Oberhollenzer F, Kiechl S, Stulnig T, Luef G, Wick G. Association of serum antibodies to heat-shock protein 65 with carotid atherosclerosis. *Lancet*. 1993;341:255–259. doi: 10.1016/0140-6736(93)92613-x
19. Wick G, Romen M, Amberger A, Metzler B, Mayr M, Falkensammer G, Xu Q. Atherosclerosis, autoimmunity, and vascular-associated lymphoid tissue. *FASEB J*. 1997;11:1199–1207. doi: 10.1096/fasebj.11.13.9367355
20. Mohanta SK, Peng L, Li Y, Lu S, Sun T, Carnevale L, Perrotta M, Ma Z, Forstera B, Stanic K, et al. Neuroimmune cardiovascular interfaces control atherosclerosis. *Nature*. 2022;605:152–159. doi: 10.1038/s41586-022-04673-6
21. Cai J, Deng J, Gu W, Ni Z, Liu Y, Kamra Y, Saxena A, Hu Y, Yuan H, Xiao Q, et al. Impact of local alloimmunity and recipient cells in transplant arteriosclerosis. *Circ Res*. 2020;127:974–993. doi: 10.1161/CIRCRESAHA.119.316470
22. Korsunsky I, Millard N, Fan J, Slowikowski K, Zhang F, Wei K, Baglaenko Y, Brenner M, Loh PR, Raychaudhuri S. Fast, sensitive and accurate integration of single-cell data with Harmony. *Nat Methods*. 2019;16:1289–1296. doi: 10.1038/s41592-019-0619-0
23. McGinnis CS, Murrow LM, Gartner ZJ. DoubletFinder: doublet detection in single-cell RNA sequencing data using artificial nearest neighbors. *Cell Syst*. 2019;8:329–337.e4. doi: 10.1016/j.cels.2019.03.003
24. Stuart T, Butler A, Hoffman P, Hafemeister C, Papalexi E, Mauck WM 3rd, Hao Y, Stoeckius M, Smibert P, Satija R. Comprehensive integration of single-cell data. *Cell*. 2019;177:1888–1902.e21. doi: 10.1016/j.cell.2019.05.031
25. Tran HTN, Ang KS, Chevrier M, Zhang X, Lee NYS, Goh M, Chen J. A benchmark of batch-effect correction methods for single-cell RNA sequencing data. *Genome Biol*. 2020;21:12. doi: 10.1186/s13059-019-1850-9
26. Cheng S, Li Z, Gao R, Xing B, Gao Y, Yang Y, Qin S, Zhang L, Ouyang H, Du P, et al. A pan-cancer single-cell transcriptional atlas of tumor infiltrating myeloid cells. *Cell*. 2021;184:792–809.e23. doi: 10.1016/j.cell.2021.01.010
27. Sun X, Wu J, Liu L, Chen Y, Tang Y, Liu S, Chen H, Jiang Y, Liu Y, Yuan H, et al. Transcriptional switch of hepatocytes initiates macrophage recruitment and T-cell suppression in endotoxemia. *J Hepatol*. 2022;77:436–452. doi: 10.1016/j.jhep.2022.02.028
28. Butler A, Hoffman P, Smibert P, Papalexi E, Satija R. Integrating single-cell transcriptomic data across different conditions, technologies, and species. *Nat Biotechnol*. 2018;36:411–420. doi: 10.1038/nbt.4096
29. Campbell KA, Lipinski MJ, Doran AC, Skaflen MD, Fuster V, McNamara CA. Lymphocytes and the adventitial immune response in atherosclerosis. *Circ Res*. 2012;110:889–900. doi: 10.1161/CIRCRESAHA.111.263186
30. Zernecke A, Winkels H, Cochain C, Williams JW, Wolf D, Soehnlein O, Robbins CS, Monaco C, Park I, McNamara CA, et al. Meta-analysis of leukocyte diversity in atherosclerotic mouse aortas. *Circ Res*. 2020;127:402–426. doi: 10.1161/CIRCRESAHA.120.316903
31. Galkina E, Kadl A, Sanders J, Varughese D, Sarembock IJ, Ley K. Lymphocyte recruitment into the aortic wall before and during development of atherosclerosis is partially L-selectin dependent. *J Exp Med*. 2006;203:1273–1282. doi: 10.1084/jem.20052205
32. Jongstra-Bilen J, Haidari M, Zhu SN, Chen M, Guha D, Cybulsky MI. Low-grade chronic inflammation in regions of the normal mouse arterial intima predisposed to atherosclerosis. *J Exp Med*. 2006;203:2073–2083. doi: 10.1084/jem.20060245
33. Houtkamp MA, de Boer OJ, van der Loos CM, van der Wal AC, Becker AE. Adventitial infiltrates associated with advanced atherosclerotic plaques: structural organization suggests generation of local humoral immune responses. *J Pathol*. 2001;193:263–269. doi: 10.1002/1096-9896(2000)9999:9999<::AID-PATH774>3.0.CO;2-N
34. Geissmann F, Manz MG, Jung S, Sieweke MH, Merad M, Ley K. Development of monocytes, macrophages, and dendritic cells. *Science*. 2010;327:656–661. doi: 10.1126/science.1178331
35. Ngo VN, Korner H, Gunn MD, Schmidt KN, Riminton DS, Cooper MD, Browning JL, Sedgwick JD, Cyster JG. Lymphotoxin alpha/beta and tumor necrosis factor are required for stromal cell expression of homing chemokines in B and T cell areas of the spleen. *J Exp Med*. 1999;189:403–412. doi: 10.1084/jem.189.2.403
36. Sautes-Fridman C, Petitprez F, Calderaro J, Fridman WH. Tertiary lymphoid structures in the era of cancer immunotherapy. *Nat Rev Cancer*. 2019;19:307–325. doi: 10.1038/s41568-019-0144-6
37. Jalkanen S, Salmi M. Lymphatic endothelial cells of the lymph node. *Nat Rev Immunol*. 2020;20:566–578. doi: 10.1038/s41577-020-0281-x
38. Libby P, Lichtman AH, Hansson GK. Immune effector mechanisms implicated in atherosclerosis: from mice to humans. *Immunity*. 2013;38:1092–1104. doi: 10.1016/j.immuni.2013.06.009
39. Cochain C, Vafadarnejad E, Arampatzi P, Pelisek J, Winkels H, Ley K, Wolf D, Saliba AE, Zernecke A. Single-cell RNA-Seq reveals the transcriptional landscape and heterogeneity of aortic macrophages in murine atherosclerosis. *Circ Res*. 2018;122:1661–1674. doi: 10.1161/CIRCRESAHA.117.312509
40. Pan H, Xue C, Auerbach BJ, Fan J, Bashore AC, Cui J, Yang DY, Trignano SB, Liu W, Shi J, et al. Single-cell genomics reveals a novel cell state during smooth muscle cell phenotypic switching and potential therapeutic targets for atherosclerosis in mouse and human. *Circulation*. 2020;142:2060–2075. doi: 10.1161/CIRCULATIONAHA.120.048378

41. Williams JW, Zaitsev K, Kim KW, Ivanov S, Saunders BT, Schrank PR, Kim K, Elvington A, Kim SH, Tucker CG, et al. Limited proliferation capacity of aortic intima resident macrophages requires monocyte recruitment for atherosclerotic plaque progression. *Nat Immunol*. 2020;21:1194–1204. doi: 10.1038/s41590-020-0768-4
42. Winkels H, Ehinger E, Vassallo M, Buscher K, Dinh HQ, Kobiyama K, Hamers AAJ, Cochain C, Vafadarnejad E, Saliba AE, et al. Atlas of the immune cell repertoire in mouse atherosclerosis defined by single-cell RNA-sequencing and mass cytometry. *Circ Res*. 2018;122:1675–1688. doi: 10.1161/CIRCRESAHA.117.312513
43. Drayton DL, Liao S, Mounzer RH, Ruddle NH. Lymphoid organ development: from ontogeny to neogenesis. *Nat Immunol*. 2006;7:344–353. doi: 10.1038/ni1330
44. Guedj K, Khallou-Laschet J, Clement M, Morvan M, Gaston AT, Fornasa G, Dai J, Gervais-Taurel M, Eberl G, Michel JB, et al. M1 macrophages act as LTbetaR-independent lymphoid tissue inducer cells during atherosclerosis-related lymphoid neogenesis. *Cardiovasc Res*. 2014;101:434–443. doi: 10.1093/cvr/cvt263
45. Tibbitt CA, Stark JM, Martens L, Ma J, Mold JE, Deswarte K, Oliynyk G, Feng X, Lambrecht BN, De Bleser P, et al. Single-cell RNA sequencing of the T helper cell response to house dust mites defines a distinct gene expression signature in airway Th2 cells. *Immunity*. 2019;51:169–184.e5. doi: 10.1016/j.immuni.2019.05.014
46. Saigusa R, Winkels H, Ley K. T cell subsets and functions in atherosclerosis. *Nat Rev Cardiol*. 2020;17:387–401. doi: 10.1038/s41569-020-0352-5
47. Nurieva R, Yang XO, Martinez G, Zhang Y, Panopoulos AD, Ma L, Schluns K, Tian Q, Watowich SS, Jetten AM, et al. Essential autocrine regulation by IL-21 in the generation of inflammatory T cells. *Nature*. 2007;448:480–483. doi: 10.1038/nature05969
48. Grogan JL, Ouyang W. A role for Th17 cells in the regulation of tertiary lymphoid follicles. *Eur J Immunol*. 2012;42:2255–2262. doi: 10.1002/eji.201242656
49. Luo S, Zhu R, Yu T, Fan H, Hu Y, Mohanta SK, Hu D. Chronic inflammation: a common promoter in tertiary lymphoid organ neogenesis. *Front Immunol*. 2019;10:2938. doi: 10.3389/fimmu.2019.02938
50. Zhang L, Wang Y. B lymphocytes in abdominal aortic aneurysms. *Atherosclerosis*. 2015;242:311–317. doi: 10.1016/j.atherosclerosis.2015.07.036
51. Sage AP, Tsiantoulas D, Binder CJ, Mallat Z. The role of B cells in atherosclerosis. *Nat Rev Cardiol*. 2019;16:180–196. doi: 10.1038/s41569-018-0106-9
52. Doran AC, Lipinski MJ, Oldham SN, Garmey JC, Campbell KA, Skaflen MD, Cutchins A, Lee DJ, Glover DK, Kelly KA, et al. B-cell aortic homing and atheroprotection depend on Id3. *Circ Res*. 2012;110:e1–12. doi: 10.1161/CIRCRESAHA.111.256438
53. Clement M, Guedj K, Andreata F, Morvan M, Bey L, Khallou-Laschet J, Gaston AT, Delbosc S, Alsac JM, Bruneval P, et al. Control of the T follicular helper-germinal center B-cell axis by CD8(+) regulatory T cells limits atherosclerosis and tertiary lymphoid organ development. *Circulation*. 2015;131:560–570. doi: 10.1161/CIRCULATIONAHA.114.010988
54. Grabner R, Lotzer K, Dopping S, Hildner M, Radke D, Beer M, Spanbroek R, Lippert B, Reardon CA, Getz GS, et al. Lymphotoxin beta receptor signaling promotes tertiary lymphoid organogenesis in the aorta adventitia of aged ApoE$^{-/-}$ mice. *J Exp Med*. 2009;206:233–248. doi: 10.1084/jem.20080752
55. Moos MP, John N, Grabner R, Nossmann S, Gunther B, Vollandt R, Funk CD, Kaiser B, Habenicht AJ. The lamina adventitia is the major site of immune cell accumulation in standard chow-fed apolipoprotein E-deficient mice. *Arterioscler Thromb Vasc Biol*. 2005;25:2386–2391. doi: 10.1161/01.ATV.0000187470.31662.fe
56. Zhao L, Moos MP, Grabner R, Pedrono F, Fan J, Kaiser B, John N, Schmidt S, Spanbroek R, Lotzer K, et al. The 5-lipoxygenase pathway promotes pathogenesis of hyperlipidemia-dependent aortic aneurysm. *Nat Med*. 2004;10:966–973. doi: 10.1038/nm1099
57. Dieude M, Turgeon J, Karakeussian Rimbaud A, Beillevaire D, Qi S, Patey N, Gaboury LA, Boilard E, Hebert MJ. Extracellular vesicles derived from injured vascular tissue promote the formation of tertiary lymphoid structures in vascular allografts. *Am J Transplant*. 2020;20:726–738. doi: 10.1111/ajt.15707
58. Graver JC, Boots AMH, Haacke EA, Diepstra A, Brouwer E, Sandovici M. Massive B-cell infiltration and organization into artery tertiary lymphoid organs in the aorta of large vessel giant cell arteritis. *Front Immunol*. 2019;10:83. doi: 10.3389/fimmu.2019.00083
59. Lund LH, Edwards LB, Kucheryavaya AY, Benden C, Christie JD, Dipchand AI, Dobbels F, Goldfarb SB, Levvey BJ, Meiser B, et al; International Society of Heart and Lung Transplantation. The registry of the International Society for Heart and Lung Transplantation: thirty-first official adult heart transplant report--2014; focus theme: retransplantation. *J Heart Lung Transplant*. 2014;33:996–1008. doi: 10.1016/j.healun.2014.08.003
60. Ostriker AC, Xie Y, Chakraborty R, Sizer AJ, Bai Y, Ding M, Song WL, Huttner A, Hwa J, Martin KA. TET2 protects against vascular smooth muscle cell apoptosis and intimal thickening in transplant vasculopathy. *Circulation*. 2021;144:455–470. doi: 10.1161/CIRCULATIONAHA.120.050553
61. Zen K, Takahara M, Iida O, Soga Y, Kawasaki D, Nanto S, Yokoi H, Matoba S; ZEPHYR Investigators. Drug-eluting stenting for femoropopliteal lesions, followed by cilostazol treatment, reduces stent restenosis in patients with symptomatic peripheral artery disease. *J Vasc Surg*. 2017;65:720–725. doi: 10.1016/j.jvs.2016.10.098
62. Alfonso F, Gonzalo N, Rivero F, Escaned J. The year in cardiovascular medicine 2020: interventional cardiology. *Eur Heart J*. 2021;42:985–1003. doi: 10.1093/eurheartj/ehaa1096
63. Georgakis MK, Bernhagen J, Heitman LH, Weber C, Dichgans M. Targeting the CCL2-CCR2 axis for atheroprotection. *Eur Heart J*. 2022;43:1799–1808. doi: 10.1093/eurheartj/ehac094
64. Peters A, Pitcher LA, Sullivan JM, Mitsdoerffer M, Acton SE, Franz B, Wucherpfennig K, Turley S, Carroll MC, Sobel RA, et al. Th17 cells induce ectopic lymphoid follicles in central nervous system tissue inflammation. *Immunity*. 2011;35:986–996. doi: 10.1016/j.immuni.2011.10.015
65. Ma X, Deng J, Han L, Song Y, Miao Y, Du X, Dang G, Yang D, Zhong B, Jiang C, et al. Single-cell RNA sequencing reveals B cell-T cell interactions in vascular adventitia of hyperhomocysteinemia-accelerated atherosclerosis. *Protein Cell*. 2022;13:540–547. doi: 10.1007/s13238-021-00904-0
66. Kyaw T, Tay C, Khan A, Dumouchel V, Cao A, To K, Kehry M, Dunn R, Agrotis A, Tipping P, et al. Conventional B2 B cell depletion ameliorates whereas its adoptive transfer aggravates atherosclerosis. *J Immunol*. 2010;185:4410–4419. doi: 10.4049/jimmunol.1000033
67. Ait-Oufella H, Herbin O, Bouaziz JD, Binder CJ, Uyttenhove C, Laurans L, Taleb S, Van Vre E, Esposito B, Vilar J, et al. B cell depletion reduces the development of atherosclerosis in mice. *J Exp Med*. 2010;207:1579–1587. doi: 10.1084/jem.20100155
68. Kosuge H, Suzuki J, Gotoh R, Koga N, Ito H, Isobe M, Inobe M, Uede T. Induction of immunologic tolerance to cardiac allograft by simultaneous blockade of inducible co-stimulator and cytotoxic T-lymphocyte antigen 4 pathway. *Transplantation*. 2003;75:1374–1379. doi: 10.1097/01.TP.0000061601.26325.82
69. Shulman Z, Gitlin AD, Weinstein JS, Lainez B, Esplugues E, Flavell RA, Craft JE, Nussenzweig MC. Dynamic signaling by T follicular helper cells during germinal center B cell selection. *Science*. 2014;345:1058–1062. doi: 10.1126/science.1257861
70. Sage PT, Sharpe AH. T follicular regulatory cells in the regulation of B cell responses. *Trends Immunol*. 2015;36:410–418. doi: 10.1016/j.it.2015.05.005
71. Srikakulapu P, Upadhye A, Rosenfeld SM, Marshall MA, McSkimming C, Hickman AW, Mauldin IS, Ailawadi G, Lopes MBS, Taylor AM, et al. Perivascular adipose tissue harbors atheroprotective IgM-producing B cells. *Front Physiol*. 2017;8:719. doi: 10.3389/fphys.2017.00719
72. Isoda K, Sawada S, Ishigami N, Matsuki T, Miyazaki K, Kusuhara M, Iwakura Y, Ohsuzu F. Lack of interleukin-1 receptor antagonist modulates plaque composition in apolipoprotein E-deficient mice. *Arterioscler Thromb Vasc Biol*. 2004;24:1068–1073. doi: 10.1161/01.ATV.0000127025.48140.a3
73. Akhavanpoor M, Gleissner CA, Akhavanpoor H, Lasitschka F, Doesch AO, Katus HA, Erbel C. Adventitial tertiary lymphoid organ classification in human atherosclerosis. *Cardiovasc Pathol*. 2018;32:8–14. doi: 10.1016/j.carpath.2017.08.002
74. van Dijk RA, Duinisveld AJ, Schaapherder AF, Mulder-Stapel A, Hamming JF, Kuiper J, de Boer OJ, van der Wal AC, Kolodgie FD, Virmani R, et al. A change in inflammatory footprint precedes plaque instability: a systematic evaluation of cellular aspects of the adaptive immune response in human atherosclerosis. *J Am Heart Assoc*. 2015;4:e001403. doi: 10.1161/JAHA.114.001403
75. Roberts WC, Moore AJ, Roberts CS. Syphilitic aortitis: still a current common cause of aneurysm of the tubular portion of ascending aorta. *Cardiovasc Pathol*. 2020;46:107175. doi: 10.1016/j.carpath.2019.107175
76. Trinidad-Hernandez M, Duncan AA. Contained ruptured paravisceral aortic aneurysm related to immunoglobulin G4 aortitis. *Ann Vasc Surg*. 2012;26:108.e1–e4. doi: 10.1016/j.avsg.2011.07.004
77. Cai J, Deng J, Gu W, Ni Z, Liu Y, Kamra Y, Saxena A, Hu Y, Yuan H, Xiao Q, et al. Impact of local alloimmunity and recipient cells in transplant arteriosclerosis. *Circ Res*. 2020;127:974–993. doi: 10.1161/CIRCRESAHA.119.316470